

See discussions, stats, and author profiles for this publication at: <https://www.researchgate.net/publication/248243159>

Kinematic modelling of the West Antarctic Rift System, Ross Sea, Antarctica

Article *in* Global and Planetary Change · December 1999

DOI: 10.1016/S0921-8181(99)00052-1

CITATIONS

37

READS

148

5 authors, including:



Martina Busetti

Istituto Nazionale di Oceanografia e di Geofisica Sperimentale

76 PUBLICATIONS 788 CITATIONS

[SEE PROFILE](#)



Dick van der Wateren

De Verwondering

38 PUBLICATIONS 998 CITATIONS

[SEE PROFILE](#)

Some of the authors of this publication are also working on these related projects:



FASTMT [View project](#)



Grythyttan Field [View project](#)



ELSEVIER

Global and Planetary Change 23 (1999) 79–103

GLOBAL AND PLANETARY
CHANGE

www.elsevier.com/locate/gloplacha

Kinematic modelling of the West Antarctic Rift System, Ross Sea, Antarctica

Martina Busetti ^{a,*}, Giacomo Spadini ^{b,1}, Frederik M. Van der Wateren ^b,
Sierd Cloetingh ^b, Claudio Zanolla ^a

^a *Osservatorio Geofisico Sperimentale, P.O. Box 2011, 34016 Opicina-Trieste, Italy*

^b *Netherlands Research School of Sedimentary Geology, Faculty of Earth Sciences, Vrije Universiteit, De Boelelaan 1085, 1081 HV Amsterdam, Netherlands*

Received 1 August 1998; accepted 1 February 1999

Abstract

In this study, we investigate the thermo-mechanical controls on the formation of the Ross Sea basin (Antarctica) and the uplift of the adjacent Transantarctic Mountains (TAM) rift shoulder, which started in the Late Cretaceous and continued until the present time. Quantitative forward modelling has been performed along three 700 to 800 km long East–West offshore profiles, extended inland to the front of the TAM. The modelling is constrained by an extensive database of multichannel seismic (MCS), refraction seismic, Ocean Bottom Seismographs (OBS), and gravity data. MCS data is tied to well stratigraphy from DSDP leg 28, CIROS-1 and MSTSS-1. Quantitative estimates of uplift of the TAM are provided by previous work on apatite fission track analysis.

We incorporate the finite strength of the lithosphere in basin formation models using the concept of the level of necking. Lateral variations of necking level and associated bulk rheological properties (with necking levels ranging from 15 km in the northernmost, to 20 km in the central and 23 km to the southernmost profiles) are required to explain the observed crustal geometries. High values of effective elastic thickness (more than 30 km) and pre-rift lithospheric thicknesses (220–230 km), indicating a cold lithosphere in a pre-rift cratonic setting, are consistent with elevation of the rift shoulder.

The western parts of the profiles appear to have unusually high stretching values without the development of oceanic crust. Inferred average values of stretching factors vary from 2.3 to 2.8, equivalent with extension in the Ross Sea of 115% to 140%. The modelling result for the uplift of the TAM predicts a late Cretaceous tectonic uplift of about 1.5 to 2.0 km, and a Cenozoic uplift of about 1.3 km restricted to southern Victoria Land. © 1999 Elsevier Science B.V. All rights reserved.

Keywords: Antarctica; Cenozoic; kinematics; modelling; seismic profiles; Ross Sea; Transantarctic Mountains

1. Introduction

The evolution of the West Antarctic Rift System (WARS) and the uplift history of the Transantarctic Mountains (TAM) rift shoulder are closely connected with the climatic and glacial history of the Antarctic continent. Questions relating to either tec-

* Corresponding author.

E-mail address: mbusetti@ogs.trieste.it (M. Busetti).

¹ Present address: ENI-AGIP Exploration and Production Division, P.O. Box 12069-20100, Milano, Italy.

tonic quiescence or activity of the rift system during the late Neogene have major implications on Antarctic Ice Sheet dynamics. Studies from one area within the TAM (the Dry Valleys, Denton et al., 1991; Sugden et al., 1995a) indicate that these mountain ranges have been a tectonically inactive passive margin since the mid Miocene, while studies from other regions (the Beardmore Glacier region, McKelvey, 1991; Webb and Harwood, 1991; Webb et al., 1984) suggest that they are an active rift flank which has undergone a fairly recent episode of tectonic uplift. This paradox could be resolved once it is realized that along-rift variations in lithospheric structure may produce contrasting behaviour of different regions within the rift flanks (Van der Wateren and Hindmarsh, 1995; Van der Wateren et al., 1996, 1999).

In this study, we address the thermo-mechanical evolution of the western part of the Ross Sea, part of

the WARS, to constrain its effect on Ross Sea rifting dynamics. A major obstacle for a detailed reconstruction of the post-rift history of this basin system has been the uncertainty range in the timing and duration of rifting, as well as the stratigraphy of the sediments in the basins. However, the quality of existing data sets is sufficient to allow us to investigate the effects of first-order spatial variation in pre-rift lithospheric structure, and to quantify the kinematics of multiple rifting.

2. Basin configuration and tectonic setting

The WARS, with an area exceeding 3000×750 km covers large parts of the Ross Sea and the Weddell Sea, (Fig. 1). It is bounded to the west by the TAM, the largest rift shoulder of the world, with

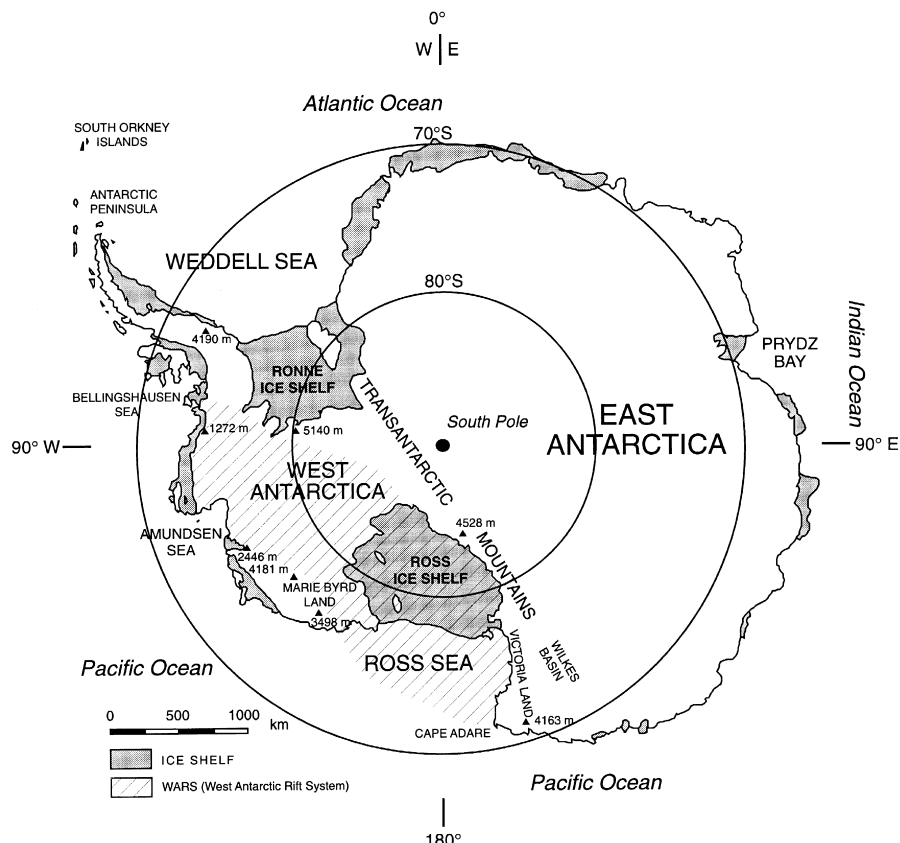


Fig. 1. The Antarctic continent, subdivided into the cratonic areas of East and West Antarctica, separated by the Cenozoic WARS and the TAM rift shoulder.

Table 1

Amount of denudation and tectonic uplift in different sectors of the TAM inferred from Apatite Fission Track Ages (AFTA)

Area	Place of uplift	Age of uplift (Ma)	Amount of denudation (km)	Amount of tectonic uplift (km)	Rate (m/Ma)	Erosion (km)	Reference
Northern Victoria Land	Central/Northern part	~ 50	~ 5	2.0 (Brown, 1991)	~ 200		Fitzgerald and Gleadow (1988)
Northern Victoria Land	Western part	~ 50	~ 1.2				Fitzgerald and Gleadow (1988)
Northern Victoria Land	Southeastern coast	~ 50	~ 10		~ 400a		Fitzgerald and Gleadow (1988)
Northern Victoria Land	Mount Nansen	Late Cretaceous					Balestrieri et al. (1994a)
Wilson Piedmont Glacier (SVL)	Mount Doorly	~ 55	~ 4.8–5.8		~ 100	~ 4–4.5	Fitzgerald (1992)
Wilson Piedmont Glacier (SVL)	Mount Termination (axis of max uplift)	~ 55	~ 6.3		~ 100	~ 4–4.5	Fitzgerald (1992)
Granite Harbour (SVL)	Mount England	~ 50	~ 4.5–5.5		~ 100	~ 4–4.5	Fitzgerald (1992)
Wright Valley (SVL)	Mount Doorly	~ 50	4.8–5.3	1.2 (Brown, 1991)	100±5		Gleadow and Fitzgerald (1987)
Dry Valleys (SVL)	Mount Jason	> 50		1.4 (Brown, 1991)			Gleadow and Fitzgerald (1987)
Scott Glacier (South Pole)	Mount Griffith	Early/Late K					Stump and Fitzgerald (1992)
Scott Glacier (South Pole)	Fission Wall Massif	Early/Late K					Stump and Fitzgerald (1992)

elevations of more than 5000 m, separating West Antarctica from East Antarctica. Uplift of the TAM occurred from the Late Mesozoic to Cenozoic (Table 1). The eastern flank of the Rift System (the Amundsen–Bellinghausen flank, Marie Byrd Land) is less defined comprising a graben and horst topography (LeMasurier and Rex, 1983) with some peaks at 3000–4000 m. In Marie Byrd Land, faulting and bi-modal volcanism began in the Oligocene (LeMasurier, 1990). It has been estimated that this rift flank was affected by about 2.2 km of uplift in the last 25 Ma (Behrendt et al., 1991).

Well data in the Ross Sea, DSDP Leg 28 (Hayes and Frakes, 1975), MSSTS-1 (Barrett, 1986) and

CIROS-1 (Barrett, 1989) recovered glacio-marine sediments from Middle Eocene (Hannah, 1994) to present. As none of these wells are deep enough to constrain the beginning of the rifting, different arguments have been used by different authors to infer that rifting probably started in late Mesozoic. According to Lawver et al. (1994), rifting started about 100 Ma because prior to that time the Ross Sea, the adjacent area of the Marie Byrd Land and the conjugate margin of the Campbell Plateau were arranged along the Pacific margin of Gondwana (see also Lawver and Gahagan, 1994). Fitzgerald et al. (1986) inferred a Late Cretaceous age consistent with the oldest sediments of the Great South Basin of New

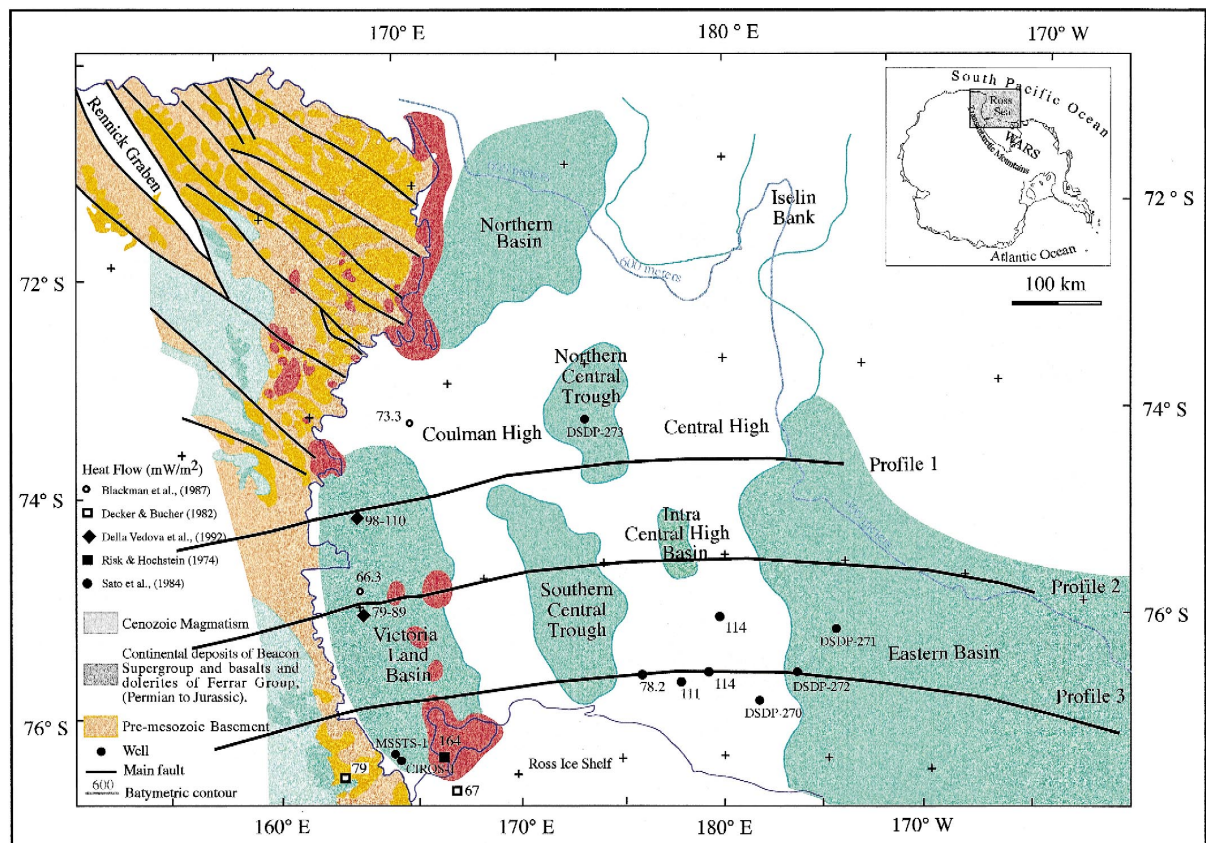


Fig. 2. Geological outline of the Ross Sea–Victoria Land area, and location of the three modelled profiles and the main sedimentary basins, the Victoria Land Basin, Central Trough and Eastern Basin, separated by structural highs. The depocentres contain late Cretaceous (?) to Palaeogene sediments (Fig. 6). The 600 m bathymetry contour approximately demarcates the shelf break of the margin. Solid lines are Precambrian to Palaeozoic faults which are reactivated during the Neogene (Salvini and Storti, 1999). Generalized rock outcrop in solid colour (Craddock, 1972). [Data from Risk and Hochstein (1974), Decker and Bucher (1982), Sato et al. (1984), Blackman et al. (1987), Della Vedova et al. (1992)].

Zealand, the conjugate margin of the eastern Ross Sea (Grindley and Davey, 1982). Apatite fission track ages from the TAM (Stump and Fitzgerald, 1992; Balestrieri et al., 1994b) indicate a first cooling episode during the Late Cretaceous. Break-up between the eastern Ross Sea and the conjugate margin of Campbell Plateau, according to Lawver et al. (1994) occurred at ~ 85 Ma. Break-up between Australia and Antarctica started around 95 Ma, but rapid separation began in the Eocene (Veevers, 1988). The western Ross Sea broke up from Tasmania, at ~ 53 Ma (Hinz et al., 1990) or at ~ 40 Ma (Lawver et al., 1992).

The TAM are regarded by some workers (Denton et al., 1991; Sugden et al., 1995a,b) as part of a tectonically stable passive margin. However, the Ross Sea is a continental shelf, which was affected by tectonic activity related to the break-up from the Campbell Plateau and from Tasmania/Australia, as well as by the Cenozoic activity of the WARS. These two processes led to the development of passive margins along the shelf break of the Northern Basin and the Eastern Ross Sea, and epicontinental basins separated by structural highs running north-south across the area towards the ocean (Fig. 2).

Fitzgerald et al. (1986) estimated a crustal extension in the Ross Embayment, using a one-layer extensional model, of about 25%–30%, or close to 200 km, by assuming a crustal thickness of 35–40 km prior to rifting (similar to that in East Antarctica) and a present-day average crustal thickness of 25–30 km. In the Victoria Land Basin (VLB), actual extension may be as much as 50%, with possibly as much as 70% beneath the central rift. Lawver and Scotese (1987), in their Gondwana reconstruction, assumed that the crust between East Antarctica and Marie Byrd Land has undergone as much as 100% extension.

3. Uplift and denudation of the TAM: previous models and constraints

In southern Victoria Land, apatite fission track analyses produced evidence of episodic denudation in different blocks of the TAM, from the Cretaceous to the Cenozoic (Table 1) (Fitzgerald, 1994). Differential block movements have been active along the

TAM front (Fitzgerald, 1992, 1994; Stump and Fitzgerald, 1992) providing different amounts of uplift at different times.

The tectonic history of northern Victoria Land appears to be quite different. Denudation of the area started at around 50 Ma (Fitzgerald and Gleadow, 1988). The amount of denudation varies from 5 km in the central and northern parts of northern Victoria Land, to 3–4 km in the western part, whereas to the southeastern coast denudation has been estimated to be about 10 km (Fig. 3). An episode of late Cretaceous denudation has been recognized in the area between Drygalski Ice Tongue and Mt. Melbourne (Balestrieri et al., 1994a).

Tonarini et al. (1995) point out that the seemingly young fission track ages in parts of northern Victoria Land may be the result of rift-related thermal events in the coastal area of Northern Victoria Land, between Campbell and Mariner Glaciers (Fig. 2). They suggest that the thermal anomaly produced by the relatively large plutons in this region may have reset the apatite fission-track systems in the surrounding rocks. Thus, early Eocene denudation inferred by Fitzgerald and Gleadow (1988) could reflect the age of Cenozoic intrusions. In other sectors of the TAM, not affected by Cenozoic igneous activity, major denudation events are recorded at late Cretaceous time (Fitzgerald and Gleadow, 1988; Stump and Fitzgerald, 1992; Balestrieri et al., 1994a), associated with the Early Rift Phase of the Ross Sea.

Different hypotheses have been proposed to explain the uplift of the TAM. Smith and Drewry (1984) attributed the uplift to the delayed effects of an anomalously hot asthenosphere forming under West Antarctica during the Late Cretaceous, moving toward the East Antarctic craton.

Fitzgerald et al. (1986) proposed a simple shear model with a shallow crustal penetrative detachment zone dipping westward beneath the TAM front. The localisation and asymmetry of this detachment zone and its unusually deep level expression are attributed to a profound crustal anisotropy inherited from an early Palaeozoic collision along the present site of the mountain range. Geochemical studies (Kalamardis and Berg, 1991; Kalamardis et al., 1987) indicate that the composition of the lower crust under the Ross Sea is quite different (lower in silica and more basic) from that under the TAM,

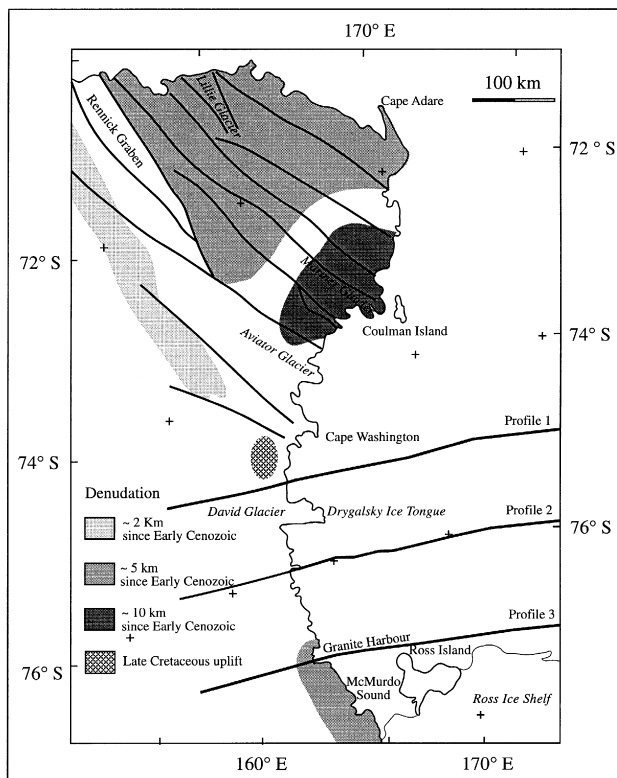


Fig. 3. Tectonic sketch map of Victoria Land (modified after Capponi et al., 1993, and Balestrieri et al., 1994b) with amount of denudation based on apatite fission track data (Gleadow and Fitzgerald, 1987; Fitzgerald and Gleadow, 1988; Fitzgerald, 1992; Balestrieri et al., 1994a).

suggesting a discontinuity and presumable suture (probably Early Palaeozoic or Precambrian age) in the lower crust between the TAM and the Ross Embayment.

Stern and Ten Brink (1989) and Stern et al. (1992) considered the uplift as the result of: (1) thermal uplift due to the advance of the low-density mantle of West Antarctica 50 km beneath the East Antarctic Plate during the last 70 Ma; (2) regional isostatic rebound following erosion of the mountain ranges; and (3) isostatic uplift of the footwall of a major normal fault across the lithosphere, and subsidence of the hanging wall (Stern et al., 1992). Ten Brink and Stern (1992) suggest that underplating of the crust may also explain some of the uplift of the margins, although the link between volcanism and permanent uplift is unclear.

On petrological evidence, Berg et al. (1989) argue that part of the uplift of the TAM has been thermally driven. The thermo-barometry yields very high tem-

perature (900°C–1000°C) in the middle and lower crust. These high temperatures and the shape of the geotherm clearly indicate that advection rather than conduction was the dominant heat-transfer mechanism in the lower and middle crust of this rift environment. The lower crust of the Ross Embayment appears to consist of extremely basic layered cumulates, many of which are ultramafic (Berg, 1991). Therefore, the geophysically determined base of the crust may actually represent an intra-crustal transition from mafic to ultramafic cumulates (Berg et al., 1989). The absence of associated inclusions of mantle lherzolite at Ross Embayment sites indicates that these ultramafic cumulates come from the lower crust and not from “pockets” in the upper mantle (Berg et al., 1989).

Heat flow in the Drygalski Basin (98–100 mW/m²), and in the Terror Rift (79–89 mW/m²) (Fig. 2) is twice the normal value, and appears to be a regional feature related to Cenozoic rifting and

flank uplift (Della Vedova et al., 1992). High heat flow is consistent with petrological studies suggesting very high geothermal gradients in the upper crust, $60^{\circ}\text{C}–100^{\circ}\text{C}/\text{km}$ (Berg, 1991).

Several authors regard the anomalous thermal conditions over the entire Ross Embayment as indicators of high temperatures at shallow depths mainly in the young rift areas. Uplift of the TAM is then explained by a thermal plume mechanism (Behrendt et al., 1991; Behrendt, 1999). They conclude that the reduced crustal thickness, high tectonic subsidence, rift related volcanism affecting the VLB, and the presence of flexural-type features in the wider Ross Sea rift area (Stern and Ten Brink, 1989) are all in favour of a thermal origin for the uplift of the TAM (Della Vedova et al., 1992). On the other hand, the small volume of magmatic material present in the region is difficult to fully reconcile with the mantle

plume hypothesis (P. Armienti, personal communication).

Berg (1991) suggested that the extremely high geothermal gradient requires an active continental-rifting environment and that simple drifting of the lithosphere over passive, previously heated asthenosphere (Smith and Drewry, 1984) would not elevate lower crustal temperatures and would not explain the very high heat flow.

Van der Beek et al. (1994) modelled the uplift of the TAM of the last 60 Ma with a kinematic model including lithospheric flexure and necking (Kooi et al., 1992). This study indicated that flexural uplift, as a result of lithospheric necking (necking depth $z_c = 30$ km), could be a plausible mechanism even in the presence of a partly thermal support of the TAM. The strongly negative residual isostatic anomalies over the Ross Sea basins (see Fig. 4) suggest that the

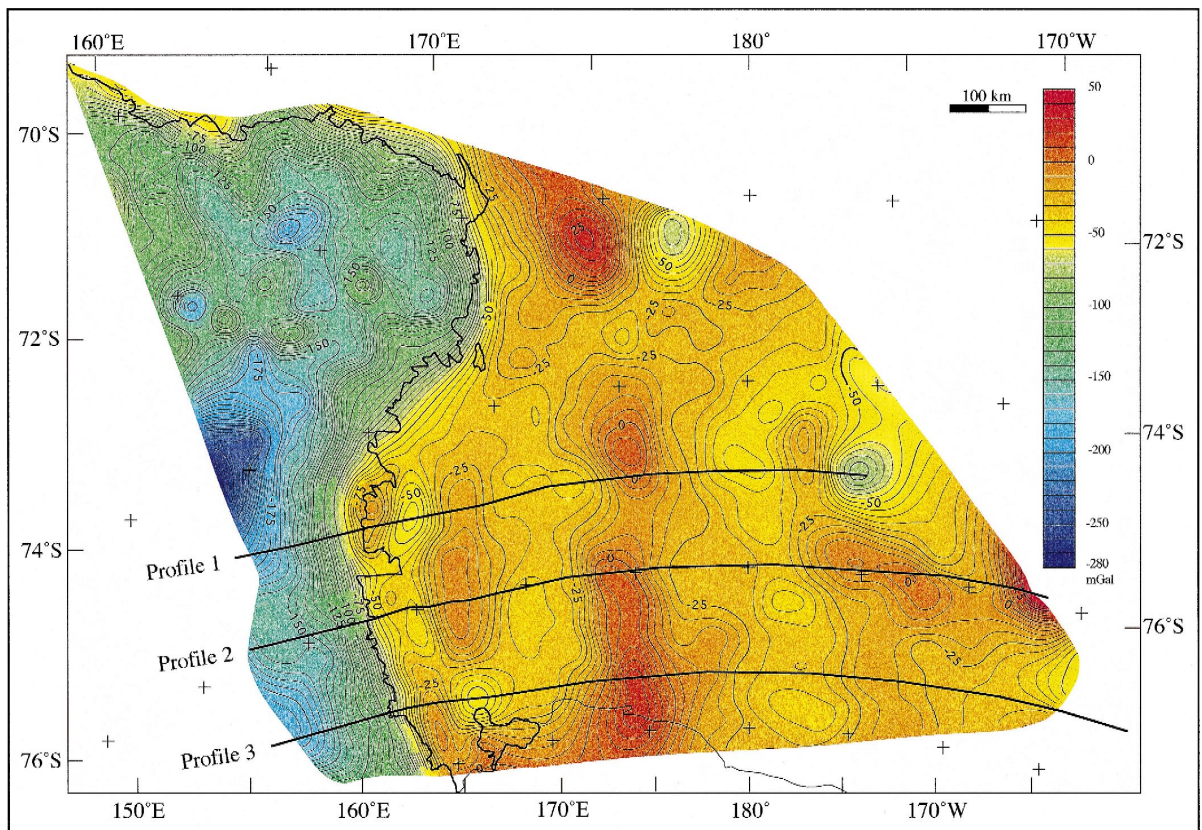


Fig. 4. Gravity map obtained merging offshore Free Air Gravity Anomaly data (Zanolla et al., 1995) and onshore Bouguer Gravity Anomaly data (Reitmayer, 1994). Contour interval is 5 mgal.

whole system is in an upward state of flexure with a strong component of mechanically supported uplift. Modelling shoulder uplift using only thermal uplift requires an excessive mantle thinning (Van der Beek et al., 1994), leading to strongly negative free air anomalies (about -100 mgal). At the same time, this model is not capable of explaining the large subsidence in the VLB.

Considerable spread in inferred effects of elastic thickness estimates (EET) has been reported, with EET values ranging from approximately 115 km and 20 km for East Antarctica and the Ross Embayment, respectively (Stern and Ten Brink, 1989), to 40–50 km and 20 km for these areas (Van der Beek et al., 1994).

4. Topography and geology of the Ross Embayment

The Ross Sea covers an area of 750,000 km², with an average water depth of ~ 500 m. Unlike low-latitude continental shelves, the Ross Sea shelf has a reverse slope from the shelf break at about 600 m to maximum near-coastal depths of 1500 m adjacent to the TAM front (Fig. 5). The present sea floor morphology is largely shaped by Neogene advances and retreats of major ice streams following approximately SSE–NNW-trending troughs which generally do not coincide with the structural grain of the rift system.

The depocentres contain early-rift sediments probably dating from the late Cretaceous to Palaeogene (Fig. 6). Separated from them by the widespread unconformity U6 (Hinz and Block, 1984; Brancolini et al., 1995a,b; De Santis et al., 1999), Neogene sediments overlie these early-rift sediments and the basement highs. Onshore and offshore volcanic activity in the western Ross Sea dates from the mid Eocene and continues until today (Tonarini et al., 1995).

The westernmost depocentre, adjacent to the TAM, is the VLB. It measures 150×400 km, and, with a maximum sediment thickness of more than 14 km, is the deepest basin in the Ross Sea. The Terror Rift, along the central axis of the VLB, is reactivated by Cenozoic tectonic and magmatic activity. To the

east of the VLB, the Coulman High stretches from south to north across the Ross Sea, merging to the North with a topographic feature that projects into the ocean. In the northern part, west of Coulman High, lies the passive margin of Northern Basin. The Northern Basin, separated from the VLB by the Coulman High, coincides with the very prominent Polar-3 magnetic anomaly (Bosum et al., 1989). East of Coulman High, a deformed area with horsts and basins separates the southern and northern Central Trough. They are shifted about 100 km in a dextral sense with respect to each other. This dextral displacement occurs along a lineament, which parallels major NW–SE trending Neogene dextral transtension structures in the Ross Embayment (Fig. 2) (Salvini and Storti, 1999; Salvini et al., 1997). The Central High, a broad and undeformed area, terminates in the Iselin Bank at the Pacific margin. The Eastern Basin, the widest basin of the area, shallows towards Marie Byrd Land in the east. The depocentre in the Eastern Basin occurs on the inner shelf (Profile 3, Fig. 6), while the outer shelf is characterized by basement high structures, resembling the basin and range style of the western rift flank in Marie Byrd Land (LeMasurier and Rex, 1991) (Profile 1, Fig. 6).

The TAM are built of Precambrian and Palaeozoic rocks and overlain by Devonian to Triassic continental to shallow water deposits of the Beacon Supergroup. The sedimentary rocks are extensively intruded and overlain by the Jurassic Ferrar Supergroup dolerites and basalts. The only rocks younger than Beacon and Ferrar are glacial and glaciomarine deposits of the Neogene Sirius Group. Most of the mountain ranges are above 2000 m elevation with maximum elevations of more than 4000 m in mountain ranges in Victoria Land closest to the Cenozoic rift margin.

The structural grain of the TAM is dominated by NW–SE trending structures of the Palaeozoic Ross Orogeny (Fig. 2). These are inherited weakness zones which have been reactivated by late Cenozoic transtensional movement, probably connected with oceanic fracture zones between Australia and northern Victoria Land (Salvini and Storti, 1999; Salvini et al., 1997). The David Glacier, flowing out into the Drygalski Ice Tongue, occupies a very deep trough (up to 1700 m bsl). It coincides with a major tectonic

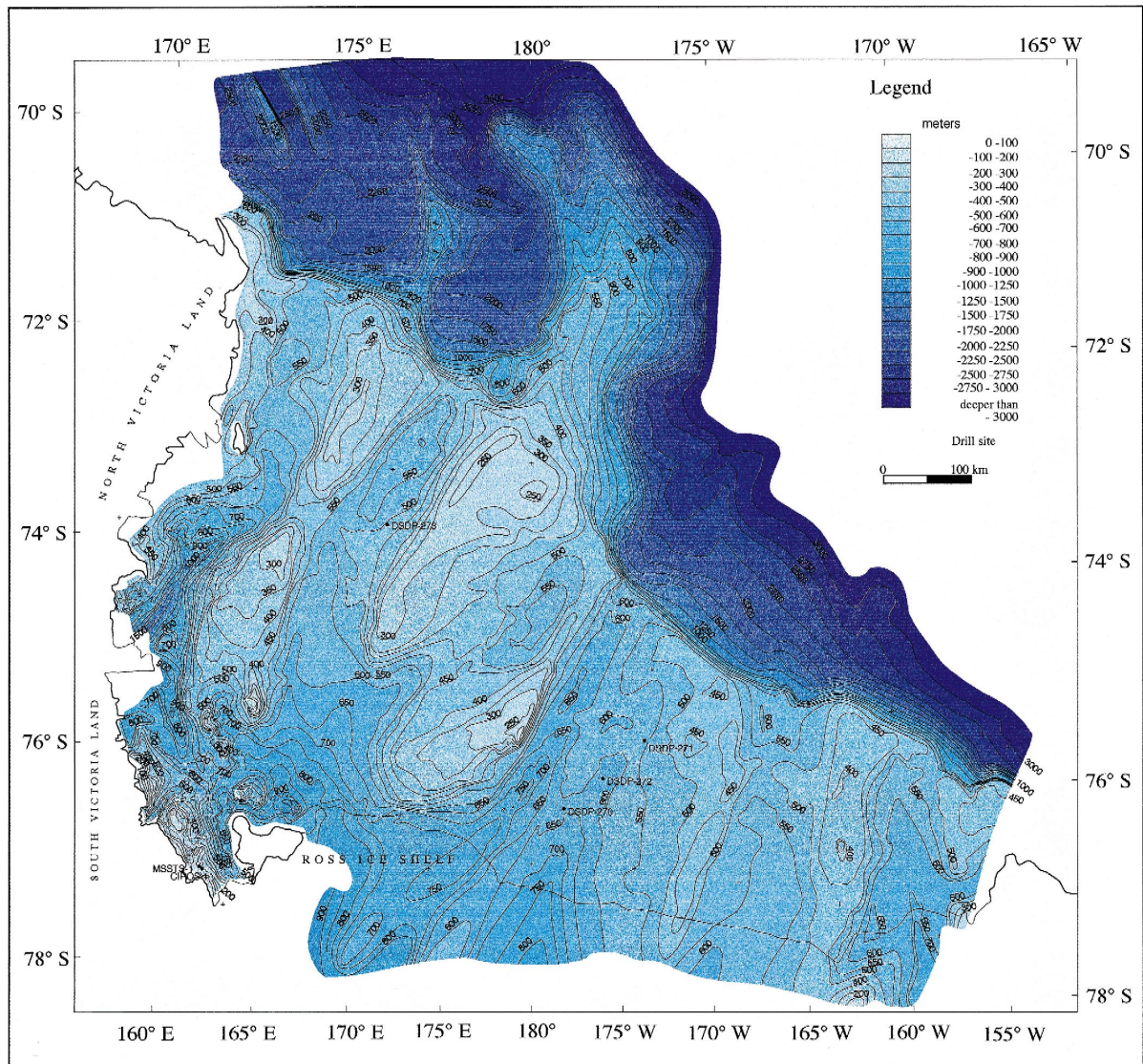


Fig. 5. Bathymetric map of the Ross Sea (Davey, 1995). Shelf break is approximately at 500–600 m. The morphological SSE–NNW basins and highs, shaped by Neogene advances and retreats of major ice stream, generally do not coincide with the structural basins and highs. Maximum water depth of 1500 m is located near the coast.

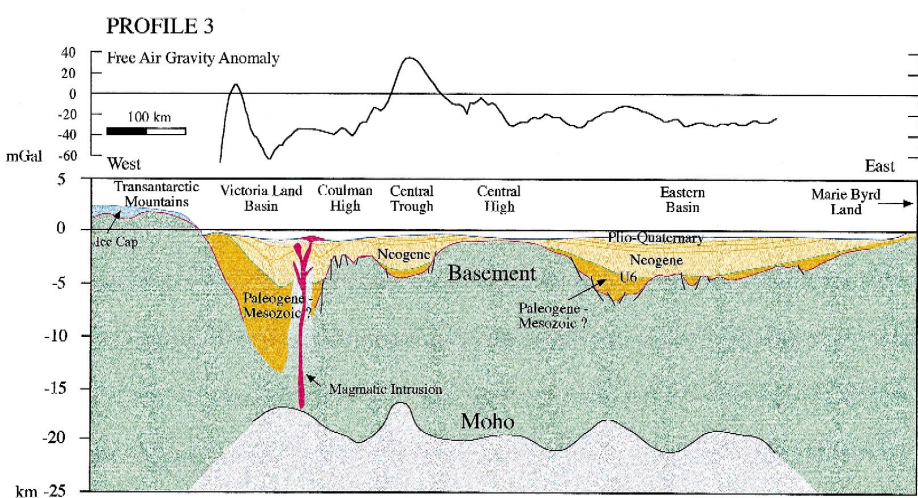
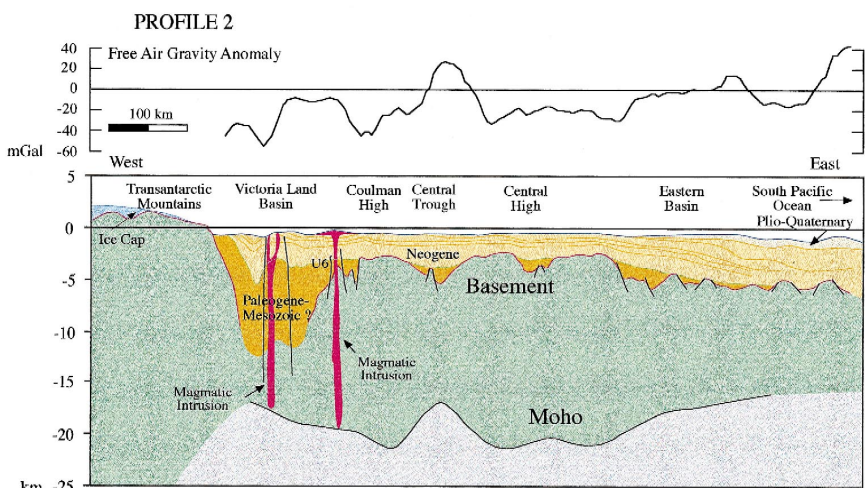
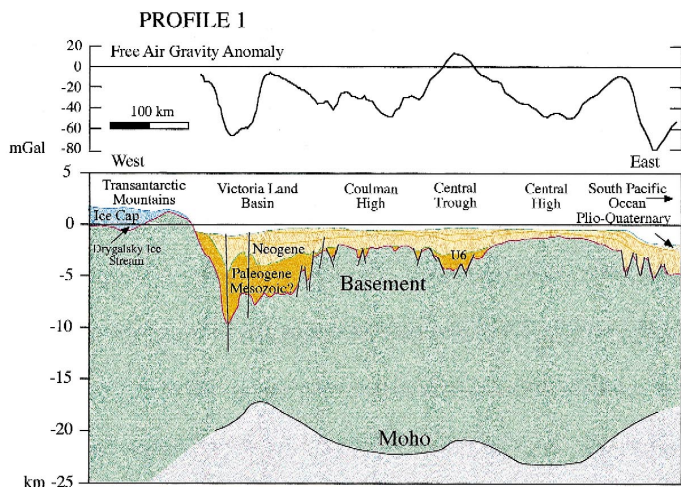
boundary separating northern and southern Victoria Land, termed the David Fault (Salvini and Storti, 1999).

To the west of the TAM is the Wilkes Basin, which is more than 500 m bsl and covered by up to 3 km of ice. Ten Brink and Stern (1992) suggest that the Wilkes Basin is a hinterland flexural basin, formed by regional isostatic response to uplift of the

TAM, although it may be the result of other processes as well.

5. Geophysical database and constraints on Moho distribution

More than 30,000 km of multichannel seismic (MCS) profiles have been acquired in the Ross Sea



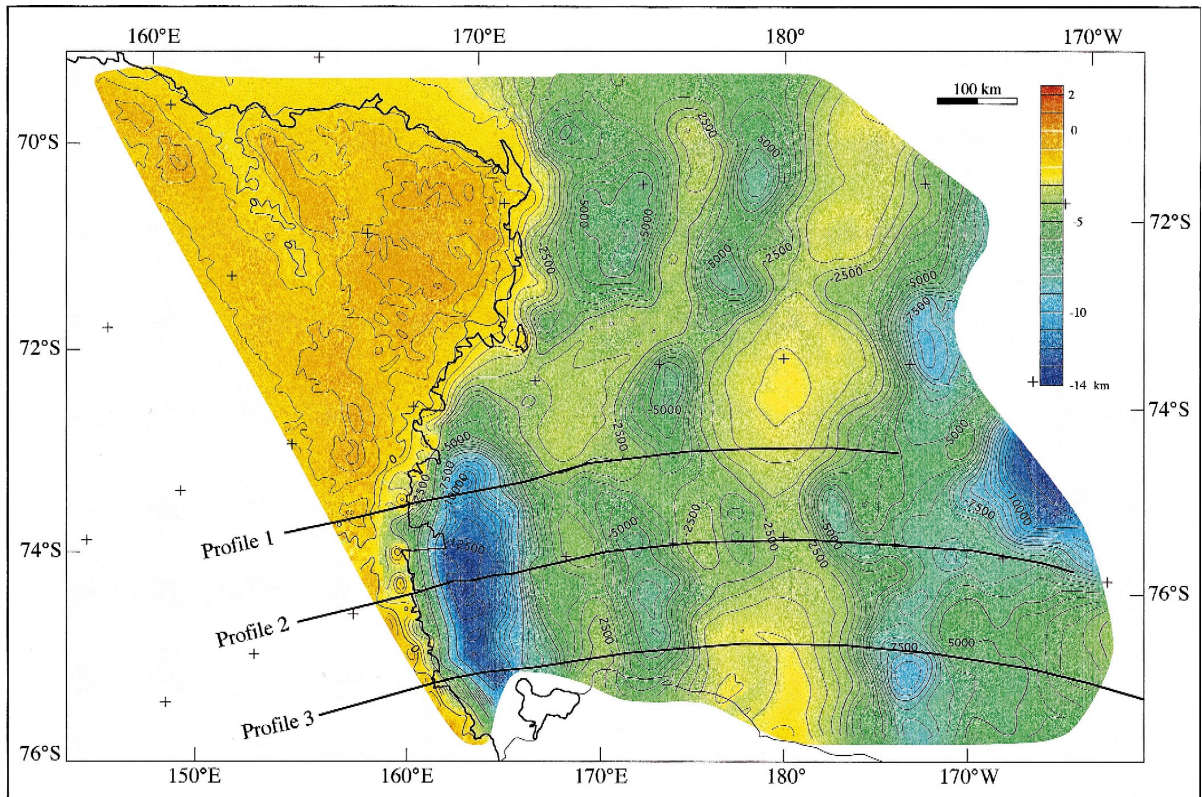


Fig. 7. Depth to basement map obtained merging offshore depth converted multichannel seismic data (Brancolini et al., 1995a,b) with onshore sub-ice topography (Drewry, 1983).

since the early 1980s by different institutes: BGR (Germany), IFP (France), JNOC (Japan), JS-MAGE (Russia), OGS (Italy) and USGS (U.S.A.). Interpretation of the multichannel data, tied to well data of DSDP Leg 28 (Hayes and Frakes, 1975), MSSTS-1 (Barrett, 1986) and CIROS (Barrett, 1989) has been carried out in the Antarctic Offshore Acoustic Stratigraphy (ANTOSTRAT) Project (Brancolini et al., 1995a,b), an international co-operative project

that involved the institutes collecting MCS data on the Antarctic margins. The Ross Sea Project produced thematic maps of the interpreted horizons, gravity and bathymetric maps (Brancolini et al., 1995a,b) (Figs. 4, 5 and 7). The depth converted basement and Moho depths provide important constraints for the modelling.

We merged depth converted basement offshore (modified after Brancolini et al., 1995a) with the

Fig. 6. Geological interpretation of the three modelled profiles. (See Fig. 2 for location). The depocentres contain early rift sediments dating from the late Cretaceous (?) to Palaeogene. Neogene glacial and glacio-marine sediments unconformably overlie these sediments and the basement highs. Interpretation of Moho depth (solid line) from refraction and OBS data (Makris et al., 1993; O'Connell and Stepp, 1993; McGinnis et al., 1985; Cooper et al., 1997; Trey et al., 1997) and from 2.5-D (Coren et al., 1994, 1997) and 2-D gravity models (Facchini, 1997).

onshore sub-ice topography (Drewry and Jordan, 1983). The basement map shows the main depocentres in the Ross Sea, with maximum depth (about 14 km) in the VLB. The onshore part of the map shows the prominent NW–SE trend related to the reactivated basement structures (Salvini and Storti, 1999).

Information about the crustal structure (Moho depth, Fig. 8) is derived from refraction seismic profiles in the Central Trough (Moho depth 17 km, Makris et al., 1993) and McMurdo Sound (21 km, McGinnis et al., 1985), and from the ACRUP refraction profile along latitude 76°S from the southern Central Trough (Cooper et al., 1997) to the Eastern Basin (Trey et al., 1997) and 2.5-D gravity modelled Moho map (Coren et al., 1994, 1997). Moho depth at the transition of the TAM to the Ross Sea, estimated

from an offshore–onshore refraction profile in the Mount Melbourne area, is about 20 km near the coast to about 25 km 40 km inland (O’Connell and Stepp, 1993), and from 2-D gravity modelled Moho of the TAM–VLB area (Facchin, 1997).

The data were compiled in the Moho map (Fig. 8) using a Laporte (1962) algorithm for gridding and contouring. Where no data was available for the modelled profile inland at the TAM front, we assumed a Moho depth of 40 km in agreement with Stern and Ten Brink (1989) and Berg et al. (1989). The Moho shape roughly mirrors the N–S trending morphology of the sedimentary basins.

Offshore Free Air (Zanolla et al., 1995) and onshore Bouguer gravity data (Reitmayer, 1994) were merged in one map (Fig. 4) using the Laporte (1962)

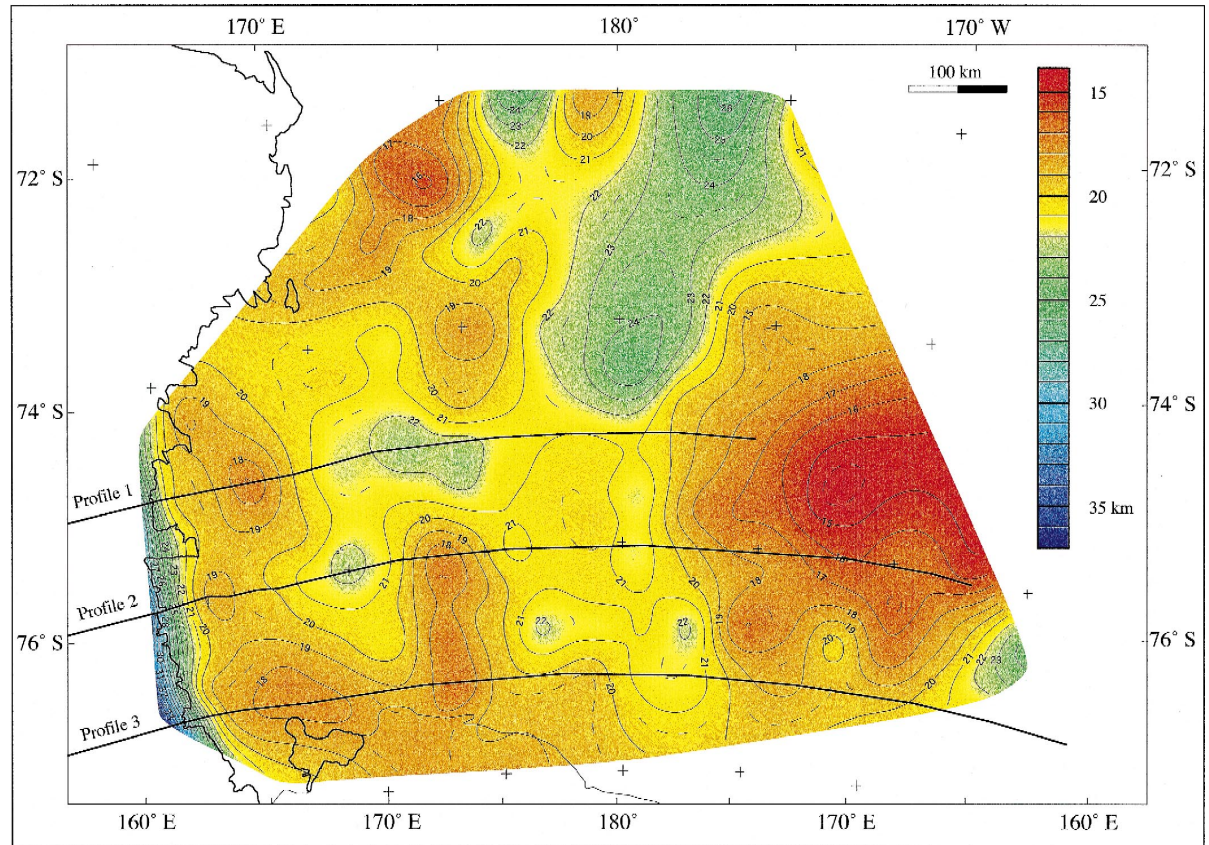


Fig. 8. Moho map (modified after Coren et al., 1994, 1997) derived from 2.5D (Coren et al., 1994) and 2D (Facchin, 1997) gravity models, and refraction data (McGinnis et al., 1985; Makris et al., 1993; O’Connell and Stepp, 1993; Cooper et al., 1997, Trey et al., 1997).

algorithm for gridding and contouring. Inland, the most conspicuous feature in the Bouguer map is a **800 km long trough-shaped anomaly** (less than -250 mgal) trending parallel to the west coast of the Ross Sea with its centre some 100 to 150 km inshore. To the north, it terminates at two major gravity lows coincident with the deeply incised Rennick and Lillie Glaciers (Reitmayr, 1994). **Offshore, free air gravity anomalies** (Zanolla et al., 1995) are dominantly negative (up to -60 mgal in the VLB). Positive anomalies, up to $+30$ mgal, occur in the Northern Basin and the northern and southern Central Trough, where the Moho depth is only 17 km.

Three depth converted E–W MCS profiles (Brancolini et al., 1995a) were chosen for our analysis (see Fig. 2 for location), running from the Victoria Land coast eastward along latitudes 75°S , 76°S and 77°S , respectively, perpendicular to the extent of the main tectonic structures (Fig. 2). These E–W profiles (Fig. 6) are obtained merging seismic lines collected by different institutes:

- Profile 1: IT90AR-61, IT90AR-79, IT89A-24 and BGR-011;
- Profile 2: USGS 407 and BGR-004;
- Profile 3: IT90AR-69, USGS 403, USGS 404, BGR-002 and IFP 207.

The profiles were extended on land to model the TAM front using basement (Drewry and Jordan, 1983; Pocknall et al., 1994; Sugden et al., 1995a) and ice topography (Drewry, 1983).

6. Tectonic modelling

We used a 2-D numerical model (Kooi et al., 1992, Spadini et al., 1997), which simulates the thermal and mechanical behaviour of a thinned lithosphere (see Table 2 for model parameters). Flexural compensation mechanisms and multiple stretching events of finite duration have been incorporated into the model.

We applied a pure shear model to the three profiles, Profile 1 along 75°S , north of the Drygalski Ice Tongue, Profile 2 along 76°S , south of the Drygalski Ice Tongue, and Profile 3 along 77°S , west of Granite Harbor (Fig. 2 and 6). The profiles were divided

Table 2
Model parameters

Parameter	Value	Definition
c	35 km	initial crustal thickness
T_0	0°C	surface temperature
T_a	1330°C	asthenosphere temperature
k	7.8×10^{-7}	thermal diffusivity
a	$3.4 \times 10^{-5^{\circ}\text{C}}$	thermal expansion coefficient
g	9.8 m s^{-2}	gravitational acceleration
r_c	2800 kg m^{-3}	surface density crustal rock
r_m	3330 kg m^{-3}	surface density mantle rock
r_s	2700 kg m^{-3}	sediment grain density
r_w	1030 kg m^{-3}	water density
f_0	0.55	sediment surface porosity
c	0.55 km^{-1}	compaction depth constant

into boxes of 10 km width. For each box, a crustal thinning factor β has been calculated, as defined by the initial crustal thickness divided by the crustal thickness observed from seismic profiles.

We assumed an **initial crustal thickness of 35 km**. **Two phases of rifting** were adopted: the first one from 100 Ma to 85 Ma (Lawver and Gahagan, 1994) and the second phase as inferred from AFTA from 60 Ma to Recent (Behrendt et al., 1991; Fitzgerald, 1992).

Model parameters are listed in Table 2. A 1330°C isotherm (adiabatic melting temperature of olivine at 100 km depth) defines the base of the lithosphere.

Transcurrent tectonics in the VLB (Salvini and Storti, 1999; Spadini et al., 1998) is incorporated by lateral heat flow (Cochran, 1983).

Sediment compaction is taken into account using an exponential porosity–depth relation:

$$\Phi_{(z)} = \Phi_0 e^{-cz} \quad (1)$$

(Slater and Christie, 1980), where Φ_0 is the sediment surface porosity, c is the compaction depth constant and z is depth.

To characterize the mechanical properties of the extending lithosphere, three parameters were incorporated: the level of necking z_c , the effective elastic thickness (EET) and the pre-rift lithospheric thickness L_o . We calibrated the model with observed lithospheric geometry to obtain the best combination of parameters for the best fit between the predicted crustal configuration and the observed geometry of the basement and the Moho. This approach was also

used to quantify the relative amounts of thinning during the Cretaceous and the Cenozoic rifting episodes, respectively, constrained by the thickness of the sediment packages deposited during these two time slices. Another goal of our modelling approach is the prediction of the amount of tectonic uplift related to the formation of the basin as a consequence of a flexurally supported rift shoulder effect.

6.1. Effective elastic thickness (EET)

The EET controls the flexural response of the lithosphere and its associated vertical motions during the syn-rift and post-rift basin evolution. The EET reflects a thermally controlled lithospheric rheology. EET is usually defined in terms of the depth of a given isotherm (Watts et al., 1982; Burov and Diamant, 1995), predicting an increase of EET with post-rift cooling.

6.2. Pre-rift lithospheric thickness

The thickness of the pre-rift lithosphere is a parameter difficult to define a priori. For this reason,

we carried out a sensitivity analysis in order to test the effects of this parameter on the final geometry of the basin. Since we consider a uniform pure shear mechanism of extension (crustal stretching = subcrustal stretching) the initial crustal thickness of the lithosphere directly controls the amount of upwelling of mantle material and thus, the regional isostatic response. This affects the regional subsidence of the plate and has a strong influence on the amount of syn-rift subsidence.

6.3. Level of necking

The level of necking is a kinematic parameter reflecting the finite strength of the lithosphere during extension (Braun and Beaumont, 1989b; Weissel and Karner, 1989; Kooi et al., 1992) with pronounced implications for rift shoulder development and basin-fill.

The level of necking can be defined as the level in the lithosphere which does not move vertically during extension and thinning in the absence of external forces (i.e., gravity, buoyancy forces) (Braun and Beaumont, 1989a,b). Models invoking a shallow level

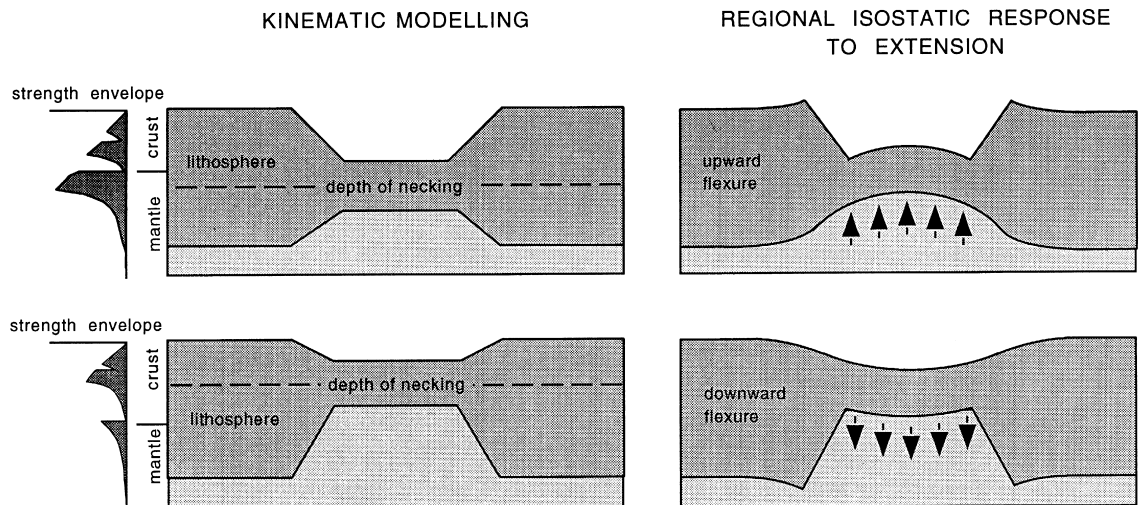


Fig. 9. Schematic illustration of the concept of lithospheric necking with a finite flexural rigidity during extensional basin formation (modified after Braun and Beaumont, 1989b; Kooi et al., 1992). Panels show the relationship between pre-rift strength distribution, level of necking incorporated into kinematic modelling and the regional response of the lithosphere to extension. Upper panel: extensional basin formation in cratonic lithosphere with lithospheric strength concentrated in the subcrustal (mantle) part of the lithosphere, leading to a deep level of necking. An upward state of flexure is induced, leading to development of a flexurally supported rift shoulder. Lower panel: extensional basin formation in Alpine thick lithosphere, characterized by a relatively shallow level of necking and downward state of flexure, resulting in flexurally downwarped rift flanks.

of necking predict a smoother basement topography and less subsidence of the basin, while a deeper level of necking predicts stronger basin subsidence and a smoother Moho shape.

Due to isostasy, a deep level of necking produces upward flexural rebound on rifting and pronounced rift shoulder uplift, whereas shallower levels of necking will reduce rift shoulder uplift, or will produce downwarped rift flanks (Fig. 9), converging ultimately towards the flexural loading model of a lithosphere with zero strength during extension (Braun and Beaumont, 1989b).

Kinematic modelling of lithospheric extension can incorporate this concept (Weissel and Karner, 1989), predicting a surface depression with a depth S :

$$S = (1 - 1/\beta) z_c. \quad (2)$$

The inferred level of necking z_c yields insight in the role of pre-rift rheology on extensional basin formation (Cloetingh et al., 1995). Several interpretations have been given to connect the level of necking to a physical boundary in the lithosphere, differing in terms of the relationships between necking depth levels in the lithosphere and the presence or absence of strong layers in the pre-rift lithosphere. These layers can support the largest stresses during extension, and therefore control the deformation of the lithosphere (Lobkovsky and Kerchman, 1991; Cloetingh et al., 1995). Kooi et al. (1992) related the level of necking with the zone of maximum lithospheric strength located at the depth of the brittle–ductile transition. According to Van der Beek et al. (1995), the level of necking represents a level in the crust where faults sole out, roughly corresponding to the level of intracrustal detachment zones, while Spadini et al. (1995) suggested that the level of necking represents the effective equivalent of the response of a multilayered rheology with a couple of strong layers in the crust and upper mantle.

7. Modelling results

We present the results of our modelling in the form of a best fit of the predicted overall crustal configuration to the available data as well as by a sensitivity analysis. To this aim, we compare pre-

dicted and observed basement and Moho distributions for the three profiles. Figs. 10–12 show the mapped top of the pre-rift basement and the position of the Moho for each of the modelled sections. As discussed, the thickness of the crust prior to rifting is difficult to measure because of the long complex tectonic history of the region. For crustal thicknesses of 40 and 45 km, the predicted relative amount of syn-rift subsidence is substantially increased, for which feature there is little evidence on seismic

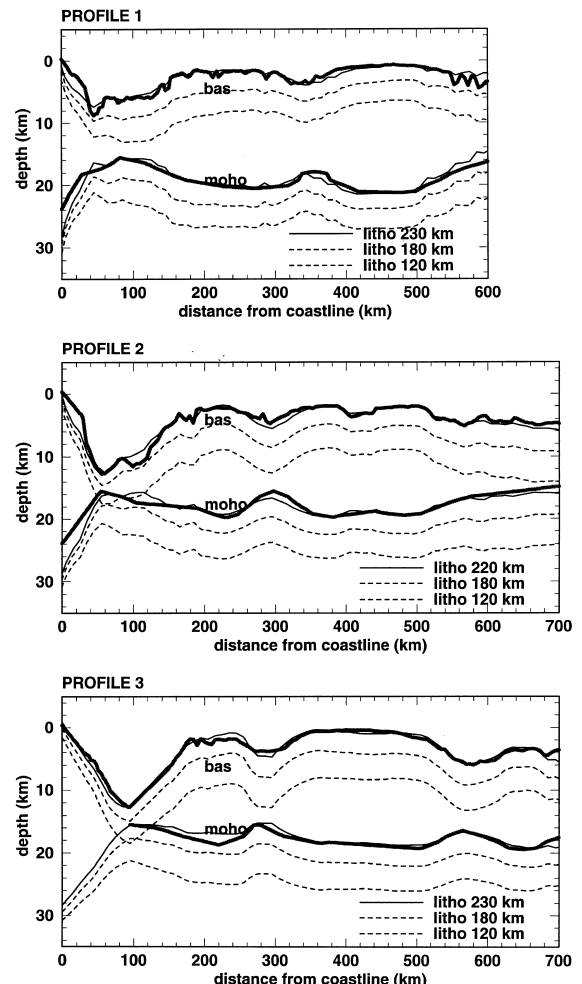


Fig. 10. Crustal configuration predicted for different pre-rift lithospheric thicknesses. Level of necking and EET assumed are from best fit models. Grey heavy line indicates observed basement and Moho. The pre-rift lithospheric thickness controls the regional subsidence/uplift of the crust. All profiles show a best fit with a “cold” model (220 or 230 km).

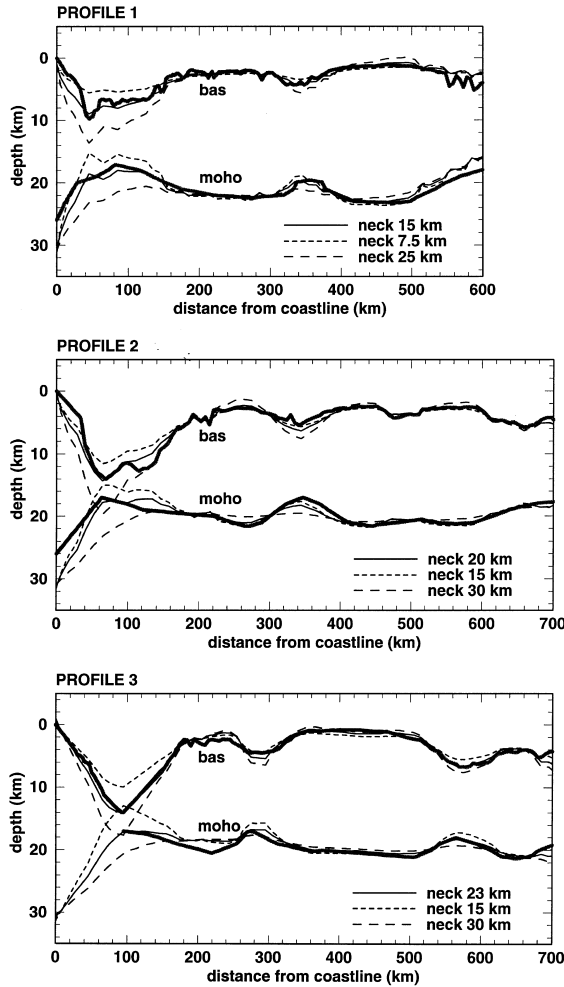


Fig. 11. Crustal configuration predicted for different depths of necking. The base of the pre-rift lithosphere (1330°C) is assumed at 230 km for Profiles 1 and 3, and at 220 km for Profile 2. Grey heavy line indicates observed basement and Moho. The depth of necking controls the difference in depth between basins and highs. The best fit level of necking (solid line) varies from 15 km in Profile 1, to 20 km in Profile 2 and 23 km in Profile 3. Lateral variation in depth of necking suggests lateral variations in mechanical properties.

profiles. We therefore adopted an initial thickness of 35 km for modelling the three profiles.

Below, we investigate the effects of variations of the following key parameters, depth of necking, EET, pre-rift lithospheric thickness, and distribution of stretching factors in space and time. This is followed by a brief discussion of the implications for syn-rift shoulder uplift.

7.1. Pre-rift lithospheric thickness

The pre-rift lithospheric thickness controls the regional subsidence of the plate. For high values of pre-rift lithospheric thickness, subcrustal thinning which produces uplift compensates subsidence due to crustal thinning. High values for initial pre-rift

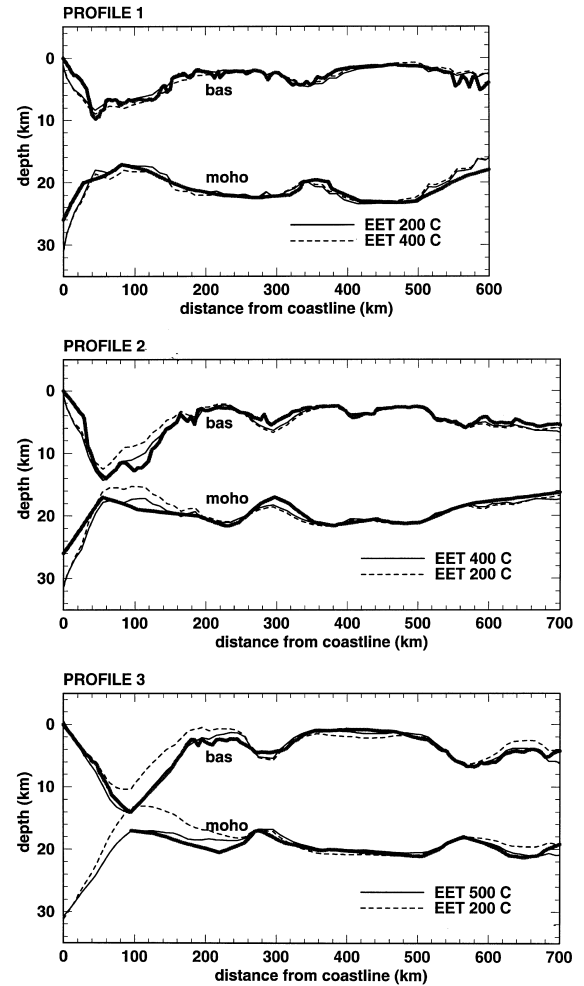


Fig. 12. Crustal configuration predicted for different EET. The base of the pre-rift lithosphere (1330°C) is assumed at 230 km for Profiles 1 and 3, and at 220 km for Profile 2. Grey heavy line indicates observed basement and Moho. The level of necking comes from the best fit model (Fig. 11). The EET controls the regional subsidence. In this model, there is a little difference between EET = 200°C and EET = 400°C . Best fit is for a 400°C EET for Profile 1 and for Profile 2, and EET = 500°C for Profile 3. High values of EET are consistent with the presence of the TAM rift shoulder.

lithospheric thickness (220 to 230 km) correspond with an initial cool lithosphere, whereas a low value for pre-rift lithospheric thickness (120 km) corresponds with a warm initial state of the extending lithosphere. Levels of necking and EET correspond with the best-fit models (Figs. 11 and 12). The results from the modelling (Fig. 10) of the pre-rift lithospheric thickness show as best fit, a “cold” lithospheric model, with the 1330°C isotherm located around 230 km (Profiles 1 and 3) and 220 km (Profile 2) in depth. The difference in predicted basement depth and Moho between the best fit “cool” model (220 to 230 km) and the other “warm” and “intermediate” pre-rift scenarios is very robust. The discrepancies between the “warm” and “intermediate” and the “cool” basement and Moho shapes, particularly under the Ross Sea basins are much higher than any possible error in the observations. Note that the differences between the “cold” and the “warm” models are large, not only at the margins, where boundary conditions (e.g., plumes, not taken into account in our modelling) can play a substantial role, but also along the entire transects.

7.2. Level of necking

Adopting pre-rift lithospheric thicknesses of 230 km (base at 1330°C) for Profiles 1 and 3, and 220 km for Profile 2 (see Fig. 10), we have varied the level of necking from shallow (7.5 to 15 km), intermediate (15 to 23 km), to deep levels (25 to 30 km). As illustrated in Fig. 11, the level of necking has a pronounced influence on the syn-rift subsidence of the Ross Sea basins, directly controlling the difference in depth between highs and basins. The crustal configuration predicted for different levels of necking, shows a progressive southward deepening.

The best fit for the northernmost Profile 1 is obtained with a necking depth of 15 km, whereas in the southern part of the basin the necking depth appears to become deeper, converging to values of 20 km and 23 km for Profiles 2 and 3, respectively. In all profiles, the VLB appears to be the area that is most sensitive to necking depth variations. Modelling results indicate a lateral variation in depth of necking that produces the best fit with basement and Moho topographies. E-W variations of necking ap-

pear to be present as well. In the Southern Central Trough (Profiles 2 and 3) the local best-fit level of necking seems to be shallower than the regional basinwide level of necking. The local best fit for Profile 2 is 15 km while the regional one is 20 km. Similarly, in Profile 3 the local best fit is again 15 km and the regional one is 23 km. Lateral variation in necking depths suggests lateral variation in mechanical properties of the lithosphere during extension.

The differences in predicted basement and Moho depths between the best-fit models and the other considered scenarios vary between 4 and 5 km near the centre of the VLB (Fig. 11), which is larger than possible errors in the observations.

7.3. EET

Fig. 12 illustrates the effects of variations in effective elastic plate thickness on predicted crustal configurations along Profiles 1, 2 and 3. Adopting a pre-rift lithospheric thickness of 230 km for Profiles 1 and 2, and 220 km for Profile 2, and best-fit necking depths (see Fig. 10), we display crustal configurations for EET values controlled by isotherms of 200°C, 400°C and 500°C (Fig. 12). The models appear to be relatively insensitive to this variable: different isotherms tested do not show significant variation of the predicted regional subsidence. Like for the level of necking, variations in the EET parameter have a most pronounced effect for the VLB where it appears to be possible to discriminate between the 400°C and 200°C EET. The best fit is obtained for an EET corresponding with an isotherm of 400°C in Profiles 1 and 2, and 500°C in Profile 3.

Adopting the base of the lithosphere at an isotherm of 1330°C, the effective elastic thickness before the onset of rifting corresponds to values of 33 to 86 km for EETs corresponding with isotherms of 200°C and 500°C, respectively (see Table 3).

7.4. Distribution of stretching factors

The total stretching factors, which we calculated, have been produced by the two main phases of rifting (100 to 85 Ma and 60 Ma to Recent). The total thinning factor is given by the products of the

Table 3

Summary of model results

L_0 : pre-rift lithospheric thickness, z_c : necking depth, EET: effective elastic thickness, β : stretching factor, $\beta = \beta_1 * \beta_2$

	L_0 (km)	z_c (km)	EET°C (km)	β_1	β_2	β
Profile 1	230	15	400 (69)	1–3	3.5	2.3
Profile 2	220	20	400 (66)	1–4	> 5	2.8
Profile 3	230	23	500 (86)	1–3	> 5	2.4

two partial thinning factors, $\beta = \beta_1 * \beta_2$. Our modelling indicates that the western part of the profiles (VLB) has been strongly affected during both the first and the second rifting phases (Fig. 13).

Along Profiles 1 and 2, the second rift phase appears to affect only the area up to 150 km from the coastline (VLB), while in Profile 3 this phase in-

volved structures more than 400 km away from the coastline (VLB, Coulman High and Central Trough), affecting the sediments in this area.

The increasing values of β in the eastern part of Profiles 1 and 2 (Fig. 13) are due to the transition to the oceanic domain. The oceanic area, not shown in profiles (Fig. 13), was taken into account in the numerical modelling in order to avoid boundary effects. For this area, we chose a maximum β factor of 5.38, which is a suitable value to simulate subsidence of oceanic crust (Keen and Beaumont, 1990).

For the first phase of rifting in all profiles, we find a maximum β value coinciding with the VLB. It reaches a value of 3 in Profile 1 and 4 in Profile 2. High β values are found in Profile 2 around 300 km, corresponding to the Central Trough and in Profile 3, around 570 km corresponding to the East-

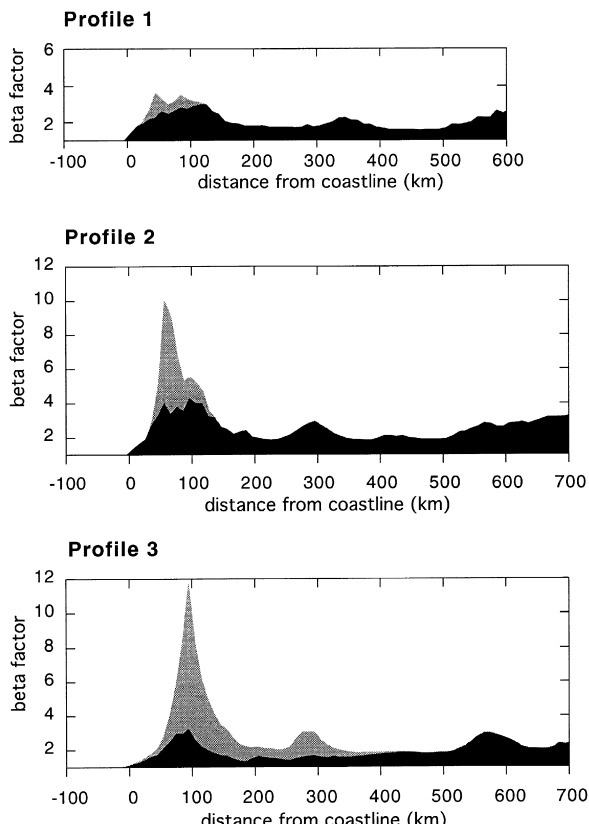


Fig. 13. Distribution of β factors (crustal thinning) of the first rifting phase (100 to 85 Ma, dark shading) and total β distribution including the second phase (60 to 0 Ma, light shading). The western part of the profiles (VLB) has been affected more intensively during both the first and the second rifting phases. In Profiles 1 and 2, the second rift phase affected only the area up to 150 km from the coastline, while in Profile 3 this phase involved structures more than 400 km away from the coastline including VLB, Coulman High and Central Trough.

ern Basin. Minimum β values are located in Profile 1 between 200 and 300 km and between 400 and 500 km corresponding to the Coulman High and Central High, respectively. In Profile 2, minimum β values of about 2, like in Profile 1 are located around the Coulman and Central Highs. In Profile 3, the location of the minimum β value is again at the Coulman and Central Highs, but is less than 2 for the Coulman High. For the second rifting phase, stretching is concentrated in the western sector, with very high values of β : 3.5 in Profile 1, more than five in the same area in the other profiles, and up to 10 in the central VLB. Average β values of about 2.3 for Profile 1, 2.8 for Profile 2 and 2.4 for Profile 3, correspond to a total extension of about 115%–140% in the Ross Sea.

7.5. Tectonic uplift of the rift shoulder

Fig. 14 shows two predicted TAM surfaces, the surface at 60 Ma, and at the present time, adopting the estimates of pre-rift lithospheric thickness, necking depth, EET and stretching distribution listed in Table 3. In all profiles, the first rifting phase produces a tectonic uplift ranging from 1500 to 2000 m. As our models focused on the controls of pre-rift lithospheric mechanical properties on the kinematics of basin formation, we refrained from modelling the post-rift subsidence and associated shoulder erosion. As demonstrated by a comparison between a predicted syn-rift shoulder topography and current topography, considerable inland migration of the rift shoulder has occurred since its formation. This is consistent with inferences from fission track studies.

In Profiles 1 and 2, the two surfaces coincide, indicating no tectonic uplift in these parts of the TAM during the last 60 Ma. Cenozoic tectonic uplift is indicated in Profile 3 with a maximum value of about 1300 m, about 15 km inland from the coast.

Apatite fission track data from southern Victoria Land (Fitzgerald, 1992), indicate 6 km of maximum total denudation and 4.5 km of erosion (Table 1) about 15–20 km inland from the coast, while Brown (1991), backstacking the fission track data, calculated at 1.2–1.4 km of tectonic uplift. The backstacked value is consistent with our model prediction along Profile 3 (Fig. 14), where a tectonic uplift of about 1.3 km has been estimated for the second phase of rifting. Our prediction of Cenozoic tectonic

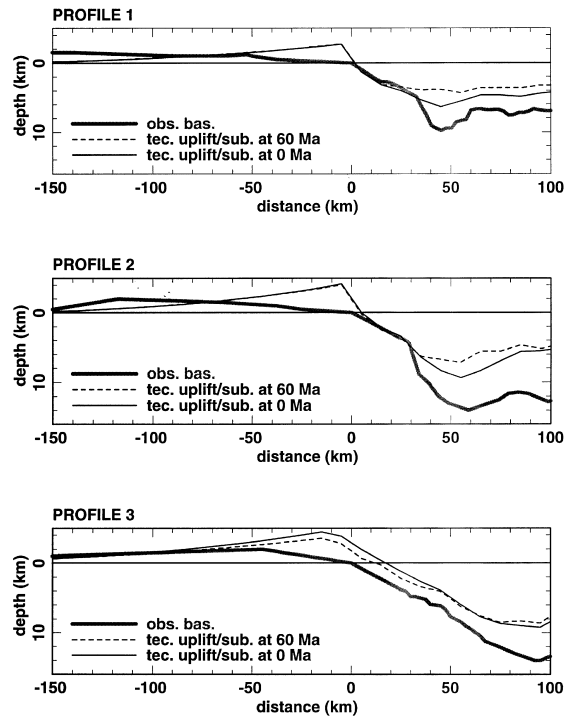


Fig. 14. Prediction of tectonic uplift of TAM up to 60 Ma and up to the present time. In all profiles, the first rifting phase produces uplift ranging from 1500 to 2000 m. The second rifting phase produces uplift only in Profile 3, with a maximum of ~1300 m. In Profile 1 and 2, the two surfaces coincide, indicating no tectonic uplift in these areas during the last 60 Ma. Differences between elevation of the observed and the predicted rift shoulder are due to erosion.

uplift does not preclude a thermal component in the evolution of the TAM.

Our modelling corroborates previous findings that the presence of marked rift shoulder topography in the TAM area appears to be a combined result of strong pre-rift lithosphere and deep levels of necking and substantial erosion, leading to strong erosion induced rebound of the rift shoulder (Van der Beek et al., 1994).

8. Discussion

Our modelling (Fig. 10) yielded similar values of best-fit pre-rift lithospheric thicknesses for all three profiles ranging from 220 to 230 km. This suggests that the pre-rift lithosphere has a fairly homogeneous

structure along the strike of the rift. This relatively large pre-rift lithospheric thickness indicates that rifting started in a cold cratonic lithosphere. These results are compatible with the estimate of a 150–250 km thermally thick lithosphere at the TAM front (Ten Brink and Stern, 1992).

The three profiles do not show significant EET variations. In the eastern area of the Ross Sea, pre-rift EETs range from 30–35 km to 66–86 km for isotherms of 200°C and 400°C–500°C, respectively. In the western sector, the EET is better constrained, yielding an EET corresponding with an isotherm of 400°C to 500°C. Stern and Ten Brink (1989) estimated an effective elastic thickness of 19 ± 5 km in the Ross Sea. Van der Beek et al. (1994), using models where the EET is defined by the 400°C–450°C isotherm, found EETs ranging from ~ 20 km within the basin to more than 40–50 km inland, for the period around 60 Ma. Flexural rigidities corresponding with these values range from 7.1×10^{22} to $5.7\text{--}11.1 \times 10^{23}$ Nm, respectively. These results suggest a thermal event, reducing the EET, during the first rifting phase.

The best fit solution for variations in necking level varied from 15, 20 to 23 km from the northern to the southern profiles. These values are regional solutions, but in all profiles a shallower level of necking appears to give a better fit for the Central Trough, which is the shallowest of the Ross Sea basins. This shows that lateral variation in mechanical properties of the lithosphere produces different basin geometries. The Central Trough is the only basin with a positive gravity anomaly due to the shallow Moho (supported by gravity as well as refraction data) underlying a relatively thin sedimentary sequence. The average necking depth values suggest that even if the TAM are partly flexurally supported, thermal effects have contributed to uplift of the flank.

The Ross Sea lithosphere shows a striking variation in mechanical properties. Anomalously high β factors, up to 10, have been inferred for the VLB. An average β value of 2.3 to 2.8 leads to an extension of about 115%–140% in the Ross Sea area. High values of β have been used by Van der Beek et al., 1994, to model the rift shoulder of the TAM, and high β values ($\beta > 5$) have been calculated for other rifts.

In the Ross Sea, the calculated amount of stretching cannot be resolved on the seismic lines. In several extensional basins and passive margins, such as the Gulf of Lions (Burrus, 1989) and the North Sea basin (Ziegler, 1983; White, 1990), the amount of upper crustal extension as measured from normal faults offset is about two times smaller than the inferred and observed amount of crustal thinning.

Petrological studies in southern Victoria Land (Berg, 1991) suggest that the geophysically-determined base of the crust may actually represent an intra-crustal transition from mafic to ultramafic cumulates, so the real Moho could be deeper and consequently the amount of vertical stretching lower than calculated. Part of the TAM uplift can be attributed to advection in the lower and middle crust (Berg et al., 1989), while associated material flow from the VLB may have reduced crustal thickness of the basin. (See also Burov and Cloetingh, 1997, for a discussion of the feedback of rift shoulder erosion and lower crustal flow.)

The modelled flank uplift shows a Cretaceous tectonic uplift of 3–4 km in all profiles. In Profiles 1 and 2, tectonic uplift has been predicted for the Cretaceous only. This agrees well with AFTA data from the area of Profile 1, north of the David Glacier/Drygalski Ice Tongue, indicating only Cretaceous cooling (Balestrieri et al., 1994a,b).

The area around the David Glacier has a low relief topography (max. elevation 2300 m) compared to the southern and northern areas (max. elevation > 4000 m) where Cenozoic uplift has been recognized. This area, informally named the Prince Albert block (van der Wateren et al., 1996), is a topographic and structural low between the Dry Valleys block and northern Victoria Land. Field observations and cosmogenic isotope measurements indicate that this area has remained low until the late Neogene, when valley downcutting into a Cretaceous/Cenozoic erosion surface began. A combination of erosional rebound and tectonic uplift produced the present topography of isolated nunataks (remnants of the elevated erosion surface) separated by deep glacial valleys (van der Wateren et al., 1996, 1999). Differential movement of crustal blocks may also be the result of Neogene transtension in the Ross Embayment (Van der Wateren et al., 1999; Wilson, 1999; Salvini and Storti, 1999).

9. Conclusions

Results from lithospheric modelling suggest that Ross Sea rifting affected a cold cratonic lithosphere with a pre-rift lithospheric thickness of approximately 230 km. Modelling of the EET shows that rifting features are not very sensitive to this parameter in the basin area. EET ranges from 30–35 km to 66–86 km. Only in the VLB, it is possible to constrain the EET value to the 500°C isotherm.

Estimates of β factors and the amount of extension for the two phases of rifting indicate that the first phase of rifting affected the entire area and that the second phase was confined to the western sector, in agreement with seismic interpretation. Thinning factors are quite high (up to 10 in the VLB): average β values of 2.3 to 2.8 (from Profile 1 to Profile 3) produced 115 to 140% extension in the Ross Sea area from the Late Cretaceous to Recent.

Lateral necking level variations from 15 km in the north to 23 km in the south indicate different mechanical properties of the lithosphere before and during rifting. Lithosphere with an intermediate value of necking can flexurally support a rift shoulder, which explains the striking topographic differences between the Dry Valleys block (west of Profile 3) and the Prince Albert block (west of Profiles 1 and 2).

Predictions of tectonic uplift of the TAM indicate a Late Cretaceous uplift of about 3–4 km, with a flexural support component, while indications of about 1.3 km of Cenozoic tectonic uplift were found only for the southern area, in agreement with back-stacked AFTA (Brown, 1991). Evidence of Late Cretaceous uplift was found in the area north of the David Glacier/Drygalski Ice Tongue (Balestrieri et al., 1994a,b), in agreement with field observations and cosmogenic isotope measurements indicating that the Prince Albert block, surrounding the David Glacier, was an area of low topography until the Late Neogene (Van der Wateren et al., 1996, 1999).

Our model results strongly indicate that differential movement of regions within the TAM rift shoulder is related to contrasting mechanical properties along the strike of the WARS. Thus, the topography presently flanking the offshore basins may have been more dynamic during the Neogene than has been suggested by Denton et al. (1991) and Sugden et al.

(1995a,b). Different regions show a different response to late Neogene transtension and to varying rates of glacial erosion. This explains why some regions within the TAM rift shoulder may have been topographically stable since the mid Miocene while others have experienced late Neogene surface uplift (Van der Wateren and Hindmarsh, 1995; Van der Wateren et al., 1996, 1999).

References

- Balestrieri, M.L., Bigazzi, G., Ghezzo, C., Lombardo, B., 1994a. Fission track dating from Granite Harbor Intrusive Suite and uplift-denudation history of the Transantarctic Mountains in the area between the Mariner and David Glaciers (Northern Victoria Land, Antarctica). In: Proceedings of the Fourth Meeting Earth Sciences in Antarctica, Siena (Italy) 3–5 February 1993. *Terra Antarct.* 1/1, 82–87.
- Balestrieri, M.L., Bigazzi, G., Ghezzo, C., Lombardo, B., 1994b. A review of apatite fission track dating from Northern Victoria Land, and a first indication of a Late Cretaceous uplift phase. In: LIRA Workshop on Crustal Structure of the Transantarctic Mountains and Adjacent Ross Sea Depression, Gradisca d'Isonzo, Italy, 3–5 June 1993. ANTOSTRAT Meeting of the Ross Sea Regional Working Group, Gradisca d'Isonzo, Italy, 31 May–2 June 1993. *Terra Antarct.* 1/3, 539–540.
- Barrett, P.J. (Ed.), Antarctic Cenozoic History from the MSSTS-1 Drillhole McMurdo Sound. DSIR Bulletin 237 Science Information Publishing Centre, Wellington, 174 pp.
- Barrett, P.J. (Ed.), Antarctic Cenozoic History from the CIROS-1 Drillhole McMurdo Sound. DSIR Bulletin 245 Science Information Publishing Centre, Wellington, 254 pp.
- Behrendt, J.C., 1999. Crustal and lithospheric structure of the West Antarctic Rift System from geophysical investigations — a review. *Global Planet. Change* 23, 25–44.
- Behrendt, J.C., LeMasurier, W.E., Cooper, A.K., Tessensohn, F., Trehu, A., Damaske, D., 1991. The West Antarctic Rift System: a review of geophysical investigations. In: Contributions to Antarctic Research II. Am. Geophys. Union, Antarct. Res. Ser. 53, 67–112.
- Berg, J.H., 1991. Geology, petrology and tectonic implications of crustal xenoliths in Cenozoic volcanic rocks of southern Victoria Land. In: Thomson, M.R.A., Crame, J.A., Thomson, J.W. (Eds.), Geological Evolution of Antarctica. Proc. Fifth Int. Symposium on Antarctic Earth Sciences, Cambridge, 23–28 August 1987. Cambridge Univ. Press, pp. 311–315.
- Berg, J.H., Moscati, R.J., Herz, D.L., 1989. A petrologic geotherm from a continental rift in Antarctica. *Earth Planet. Sci. Lett.* 93, 98–108.
- Blackman, D.K., Von Herzen, R.P., Lawver, L.A., 1987. Heat flow and tectonics in the Western Ross Sea, Antarctica. In: Cooper, A.K., Davey, F.J. (Eds.), The Antarctic Margin: Geology and Geophysics of the Western Ross Sea. Earth

- Science Series 5B Circum-Pacific Council of Energy and Mineral Resources, Houston, TX, pp. 179–189.
- Bosum, W., Damaske, D., Roland, N.W., Behrendt, J.C., Saltus, R., 1989. The Ganovex IV Victoria Land/Ross sea aeromagnetic survey: interpretation of anomalies. *Geol. Jahrb.*, E 38, 153–230.
- Brancolini, G., Busetti, M., Marchetti, A., De Santis, L., De Cillia, C., Zanolla, C., Coren, F., Cooper, A.K., Cochrane, G., Zayatz, I., Belyaev, V., Knyazev, M., Vinnikovskaya, O., Davey, F., Hinz, K., 1995a. Seismic stratigraphic atlas of the Ross Sea, Antarctica. In: Cooper, A.K., Barker, P.F., Brancolini, G. (Eds.), *Geology and Seismic Stratigraphy of the Antarctic Margin*. *Antarct. Res. Ser.* 68 AGU, Washington, DC.
- Brancolini, G., Busetti, M., Marchetti, A., De Santis, L., De Cillia, C., Zanolla, C., Coren, F., Cooper, A.K., Cochrane, G., Zayatz, I., Belyaev, V., Knyazev, M., Vinnikovskaya, O., Davey, F., Hinz, K., 1995b. Descriptive text for the seismic stratigraphic atlas of the Ross Sea, Antarctica. In: Cooper, K., Barker, P.F., Brancolini, G. (Eds.), *Geology and Seismic Stratigraphy of the Antarctic Margin*. *Antarct. Res. Ser.* 68 AGU, Washington, DC.
- Braun, J., Beaumont, C., 1989a. Dynamical models of the role of crustal shear zones in asymmetric continental extension. *Earth Planet. Sci. Lett.* 93, 405–423.
- Braun, J., Beaumont, C., 1989b. A physical explanation for the relationship between flank uplifts and the breakup unconformities at rifted continental margins. *Geology* 17, 760–764.
- Brown, R.W., 1991. Backstacking apatite fission-track “stratigraphy”: a method for resolving the erosional and isostatic rebound components of tectonic uplift histories. *Geology* 19, 74–77.
- Burov, E., Cloetingh, S., 1997. Erosion and rift dynamics: new thermomechanical aspects of post-rift evolution of extensional basins. *Earth Planet. Sci. Lett.* 150, 7–26.
- Burov, E., Diament, M., 1995. The effective elastic thickness (T_e) of continental lithosphere: what does it really mean? *J. Geophys. Res.* 100, 3905–3927.
- Burrus, J., 1989. Review of geodynamic models for extensional basins; the paradox of stretching in the gulf of Lions (Northwest Mediterranean). *Bull. Soc. Geol. Fr.* 8/2, 377–393.
- Capponi, G., Casnedi, R., Castelli, D., Flöttmann, T., Jordan, H., Kleinschmidt, G., Lombardo, B., Meccheri, M., Oggiano, G., Pertusati, P.C., Ricci, C.A., Schmidt-Thomé, M., Skinner, D.N.B., Tessensohn, F., Thiedig, F., 1993. Geological and structural map of the area between the Aviator Glacier and Victory Mountains, Northern Victoria Land, Antarctica. GANOVEX-PNRA Italianartide (Editors).
- Cloetingh, S., van Wees, J.D., Van der Beek, P.A., Spadini, G., 1995. Role of pre-rift rheology in kinematics of extensional basin formation: constraints from thermomechanical models of Mediterranean and intracratonic basins. *Mar. Pet. Geol.* 12, 793–807.
- Cochran, J.R., 1983. Effects of finite rifting times on the development of sedimentary basins. *Earth Planet. Sci. Lett.* 66, 289–302.
- Cooper, A.K., Trey, H., Cochrane, G., Egloff, F., Busetti, M., Acrup Working Group, 1997. Crustal structure of the Southern Central Trough, Western Ross Sea. In: Ricci, C.A. (Ed.), *The Antarctic Region: Geological Evolution and Processes. Proceedings of the VIIth International Symposium on Antarctic Earth Sciences*, Siena 1995. Terra Antarctica Publications, pp. 637–642.
- Coren, F., Zanolla, C., Marson, I., 1994. Computation of the Moho depths from gravity data in the Ross Sea (Antarctica). In: Sünkel, H., Marson, I. (Eds.), *Proceedings of Gravity and Geoid: Joint Symposium of the International Gravity Commission and the International Geoid Commission, Symposium n. 113*, Graz (Austria), September 11–17, 1994. Springer-Verlag, pp. 278–285.
- Coren, F., Marson, I., Stoka, M., Zanolla, C., 1997. Computation of the Moho depths and geoid undulation from gravity data in the Ross Sea (Antarctica). In: Ricci, C.A. (Ed.), *The Antarctic Region: Geological Evolution and Processes. Proceedings of the VII International Symposium on Antarctic Earth Sciences*, Siena 1995. Terra Antarctica Publications, pp. 603–608.
- Craddock, C., 1972. *Geologic Map of Antarctica*, 1: 5,000,000. American Geographical Society, New York.
- Davey, F.J., 1995. Seismic stratigraphic atlas of the Ross Sea, Antarctica: bathymetry. In: Cooper, A.K., Barker, P.F., Brancolini, G. (Eds.), *Geology and Seismic Stratigraphy of the Antarctic Margin*. *Antarct. Res. Ser.* 68 AGU, Washington, DC.
- Decker, E.R., Bucher, G.J., 1982. Geothermal studies in the Ross Island–Dry Valley region. In: Craddock, C. (Ed.), *Antarctic Geoscience*. Madison University of Wisconsin Press, pp. 887–894.
- Della Vedova, B., Pellis, G., Lawver, L.A., Brancolini, G., 1992. Heatflow and tectonics of the Western Ross Sea. In: Yoshida, Y., Kaminuma, K., Shiraiishi, K. (Eds.), *Recent Progress in Antarctic Earth Science, Proceedings of the Sixth International Symposium on Antarctic Earth Science*, Saitama Japan, September 9–13, 1991. pp. 627–637.
- Denton, G.H., Prentice, M.L., Burckle, L.H., 1991. Cainozoic history of the Antarctic Ice Sheet. In: Tingey, R.J. (Ed.), *The Geology of Antarctica*. Oxford Monographs on Geology and Geophysics 17 Oxford Science Publications, pp. 365–433.
- De Santis, L., Prato, S., Brancolini, G., Lovo, M., Torelli, L., 1999. The eastern Ross Sea continental shelf during the Cenozoic and implications for the West Antarctic ice sheet development. *Global Planet. Change* 23, 173–196.
- Drewry, D.J., 1983. The surface of Antarctic Ice Sheet. In: Drewry, D.J. (Ed.), *Antarctica: Glaciological and Geophysical Folio*. Scott Polar Research Institute, Cambridge.
- Drewry, D.J., Jordan, S.R., 1983. The bedrock surface of Antarctica. In: Drewry, D.J. (Ed.), *Antarctica: Glaciological and Geophysical Folio*. Scott Polar Research Institute, Cambridge.
- Faccin, L., 1997. Structural study of Victoria Land Basin (Ross Sea, Antarctica). Thesis of Laurea at the University of Trieste, Italy, 108 pp.
- Fitzgerald, P.G., 1992. The Transantarctic Mountains of Southern Victoria Land: the application of apatite fission track analysis to a rift shoulder uplift. *Tectonics* 11, 634–662.
- Fitzgerald, P.G., 1994. Thermochronologic constraints on post-Paleozoic tectonic evolution of the central Transantarctic Mountains. *Tectonics* 13, 818–836.

- Fitzgerald, P.G., Gleadow, A.J.W., 1988. Fission-track geochronology, tectonics and structure of the Transantarctic Mountains in Northern Victoria Land, Antarctica. *Chem. Geol.* (Isotope Geosci. Section) 13, 169–198.
- Fitzgerald, P.G., Sandiford, M., Barrett, P.J., Gleadow, A.J.W., 1986. Asymmetric extension associated with uplift and subsidence in the Transantarctic Mountains and Ross Embayment. *Earth Planet. Sci. Lett.* 81, 67–78.
- Gleadow, A.J.W., Fitzgerald, P.G., 1987. Uplift history and structure of the Transantarctic Mountains: new evidence from fission track dating of basement apatite in the Dry Valley area, southern Victoria Land. *Earth Planet. Sci. Lett.* 82, 93–102.
- Grindley, G.W., Davey, F.J., 1982. The reconstruction of New Zealand, Australia and Antarctica (review paper). In: Craddock, C. (Ed.), Antarctic Geoscience. University of Wisconsin Press, Madison, WI, pp. 15–30.
- Hannah, M.J., 1994. Eocene dinoflagellates from the CIROS-1 drill hole, McMurdo Sound, Antarctica. *Terra Antarct.* 1/2, 371–372.
- Hayes, D.E., Frakes, L.A., 1975. General synthesis, deep sea drilling project. In: Hayes, D.E., Frakes, L.A. (Eds.), Initial Reports of the Deep Sea Drilling Project, Leg 28 28 US Government Printing Office, Washington, pp. 919–942.
- Hinz, K., Block, M., 1984. Results of geophysical investigations in the Weddell Sea and in the Ross Sea, Antarctica. In: Proceeding 11th World Petrol. Congr., London 1983. Wiley, New York, pp. 279–291.
- Hinz, K., Hemmerich, M., Salge, U., Eiken, O., 1990. Structures in rift basin sediments on the conjugate margins of western Tasmania, South Tasman Rise, and Ross Sea, Antarctica. In: Bleil, U., Thiede, J. (Eds.), Geological History of the Polar Oceans: Arctic versus Antarctic. pp. 119–130.
- Kalamarides, R.I., Berg, J.H., 1991. Geochemistry and tectonic implications of lower-crustal granulites included in Cenozoic volcanic rocks of southern Victoria Land. In: Thomson, M.R.A., Crame, J.A., Thomson, J.W. (Eds.), Geological Evolution of Antarctica, Proceedings of the Fifth International Symposium on Antarctic Earth Sciences, Cambridge, 23–28 August 1987. Cambridge Univ. Press, pp. 305–310.
- Kalamarides, R.I., Berg, J.H., Hank, R.A., 1987. Lateral isotopic discontinuity in the lower crust: an example from Antarctica. *Science* 237 (4819), 1192–1195.
- Keen, C.E., Beaumont, C., 1990. Geodynamics of rifted continental margins. In: Keen, M.J., Williams, G.L. (Eds.), Geology of Continental Margin of Eastern Canada. Geological Survey of Canada. *Geology of Canada* 2pp. 391–472, (also Geological Society of America, The Geology of North America, I-1).
- Kooi, H., Cloetingh, S., Burrus, J., 1992. Lithospheric necking and regional isostasy at extensional basins 1. Subsidence and gravity modelling with application to the Gulf of Lions Margins (SE France). *J. Geophys. Res.* 97, 17553–17571.
- Laporte, M., 1962. Elaboration rapide de cartes gravimétrique déduites de l'anomalie de Bouguer à l'aide d'une calculatrice électronique. *Geophys. Prospect.* 10, 238–257.
- Lawver, L.A., Gahagan, L.M., 1994. Constraints on timing of extension in the Ross Sea Region. In: LIRA workshop on crustal structure of the Transantarctic Mountains and adjacent Ross Sea depression, Gradiška d'Isonzo, Italy, 3–5 June 1993. ANTOSTRAT Meeting of the Ross Sea Regional Working Group, Gradiška d'Isonzo, Italy, 31 May–2 June 1993. *Terra Antarct.* 1/3, pp. 545–552.
- Lawver, L.A., Scotese, C.R., 1987. A revised reconstruction of Gondwanaland. In: McKenzie, G.D. (Ed.), *Gondwana Six: Structure, Tectonics, and Geophysics*. AGU Geophys. Monogr. 40, pp. 17–24.
- Lawver, L.A., Gahagan, L.M., Coffin, M.F., 1992. The development of paleoseaways around Antarctica. In: *The Antarctic Paleoenvironment: A Perspective on Global Change*. *Antarct. Res. Ser.* 56, pp. 7–30.
- Lawver, L.A., Gahagan, L.M., Cooper, A.K., 1994. Comparison of the Eastern Ross Sea with Campbell Basin. In: Cooper, A.K., Barker, P.F., Webb, P.N., Brancolini, G. (Eds.), *The Antarctic Continental Margin: Geophysical and Geological Stratigraphic Records of Cenozoic Glacial Paleoenvironments, and Sea-level Change*. *Terra Antarct.* 1/2, pp. 375–377.
- LeMasurier, W.E., 1990. Marie Byrd Land. In: LeMasurier, W.E., Thomson, J.W. (Eds.), *Volcanoes of the Antarctic Plate and Southern Oceans*. *Antarct. Res. Ser.* 48 AGU, Washington, DC, pp. 147–250.
- LeMasurier, W.E., Rex, D.C., 1983. Rates of uplift and the scale of ice level instabilities recorded by volcanic rocks in Marie Byrd Land, West Antarctica. In: Oliver, R.L., James, P.R., Jago, J.B. (Eds.), *Antarctic Earth Science, Proceedings of the Fourth International Symposium on Antarctic Earth Sciences*, University of Adelaide, South Australia, 16–20 August 1982. Australian Academy of Science, Canberra, pp. 663–670.
- LeMasurier, W.E., Rex, D.C., 1991. The Marie Byrd Land volcanic province and its relation to the Cainozoic West Antarctic Rift System. In: Tingey, R. (Ed.), *The Geology of Antarctica*. Oxford Univ. Press, Oxford, pp. 249–284.
- Lobkovsky, L.I., Kerchman, V.I., 1991. A two-level concept of plate tectonics: application to geodynamics. *Tectonophysics* 199, 343–374.
- Makris, J., Egloff, F., Orbach, S., Fritsch, J., Damaske, D., Dürbaum, H.J., 1993. Seismic study of the Central Basin of the Ross Sea, Antarctica. In: Damaske, D., Fritsch, J. (Eds.), *German Antarctic North Victoria Land Expedition 1988/89, GANOVEX V*. *Geol. Jahrb.*, E 47, pp. 277–290.
- McGinnis, L.D., Bowen, R.H., Erickson, J.M., Allred, B.J., Kremer, J.L., 1985. East–West Antarctic Boundary in McMurdo Sound. *Tectonophysics* 114, 341–356.
- McKelvey, B.C., 1991. The Cainozoic glacial record in South Victoria Land: a geological evaluation of the McMurdo Sound drilling projects. In: Tingey, R.J. (Ed.), *The Geology of Antarctica*. Clarendon Press, Oxford, pp. 434–454.
- O'Connell, D.R.H., Stepp, T.M., 1993. Structure and evolution of the crust at the transantarctic mountains — Ross Sea crustal transition: results from the Tourmaline Plateau Seismic Array of the GANOVEX V ship-to-shore seismic refraction experiments. *Geol. Jahrb.*, E 47, 229–276.
- Pocknall, D.T., Chinn, T.J., Sykes, R., Skinner, D.N.B., 1994. Geology of the Convoy Range area, southern Victoria Land,

- Antarctica. Scale 1:50.000. Institute of Geological and Nuclear Sciences geological map 11, 1 sheet +36 pp. Institute of Geological and Nuclear Sciences, Lower Hutt, New Zealand
- Reitmayer, G., 1994. The gravity map of Victoria Land, Antarctica. In: LIRA Workshop on Crustal Structure of the Transantarctic Mountains and Adjacent Ross Sea Depression, Gradisca d'Isonezo, Italy, 3–5 June 1993. ANTOSTRAT Meeting of the Ross Sea Regional Working Group, Gradisca d'Isonezo, Italy, 31 May–2 June 1993. Terra Antarct. 1/3, pp. 495–500.
- Risk, G.F., Hochstein, M.P., 1974. Heat flow at arrival heights, Ross Island, Antarctica. N. Z. J. Geol. Geophys. 17, 629–644.
- Salvini, F., Storti, F., 1999. Cenozoic tectonic lineaments of the Terra Nova Bay region, Ross Embayment, Antarctica. Global Planetary Change 23, 129–144.
- Salvini, F., Brancolini, G., Busetti, M., Storti, F., Mazzarini, F., Coren, F., 1997. Cenozoic geodynamics of the Ross Sea–Victoria Land Region, Antarctica: insight from offshore and onshore data. J. Geophys. Res. 102 (B11), 24669–24696.
- Sato, S., Asakura, N., Saki, T., Oikawai, N., Kaneda, Y., 1984. Preliminary results of geological and geophysical surveys in the Ross Sea and in the Dumont d'Urville Sea, of Antarctica. In: Proceedings of the 4th Symposium on Antarctic Geosciences 1983, National Institute for Polar Research, Tokyo. Memoirs of the National Institute of Polar Research 33, pp. 66–92.
- Sclater, J.G., Christie, P.A.F., 1980. Continental stretching: an explanation of post mid-Cretaceous subsidence of central North Sea. J. Geophys. Res. 85, 3711–3739.
- Smith, A.G., Drewry, D.J., 1984. Delayed phase change due to hot asthenosphere causes Transantarctic uplift? Nature 309, 536–538, 7 June 1984.
- Spadini, G., Cloetingh, S., Bertotti, G., 1995. Thermomechanical modeling of the Tyrrenian Sea: lithospheric necking and kinematics of rifting. Tectonics 14, 629–644.
- Spadini, G., Robinson, A.G., Cloetingh, S., 1997. Thermomechanical modelling of Black Sea basin formation, subsidence and sedimentation. In: Regional and Petroleum Geology of the Black Sea and Surrounding Region. Am. Assoc. Pet. Geol. Mem. 68, pp. 19–38.
- Spadini, G., Ben-Avraham, Z., Busetti, M., 1998. Transform-normal extension in the Victoria Land Basin (Antarctica). Rend. Fis. Acc. Lincei. 9(19), 257–269.
- Stern, T., Ten Brink, U., 1989. Flexural uplift of the Transantarctic Mountains. J. Geophys. Res. 41, 10.315–10.330.
- Stern, T., Ten Brink, U., Bott, M.H.P., 1992. Numerical modelling of uplift and subsidence adjacent to the Transantarctic Mountains. In: Yoshida, Y. (Ed.), Recent Progress in Antarctic Earth Science. pp. 515–521.
- Stump, E., Fitzgerald, P.G., 1992. Episodic uplift of the Transantarctic Mountains. Geology 20, 161–164.
- Sugden, D.E., Denton, G.H., Marchant, D.R., 1995a. Landscape evolution of the Dry Valleys, Transantarctic Mountains: tectonic implications. J. Geophys. Res. 100 (B6), 9949–9967.
- Sugden, D.E., Marchant, D.R., Potter, N., Souchez, R.A., Denton, G.H., Swisher, C.C., Tison, J.L., 1995b. Preservation of Miocene glacier ice in East Antarctica. Nature 376, 412–414.
- Ten Brink, U., Stern, T., 1992. Rift flank uplift and Hinterland Basins: comparison of the Transantarctic Mountains with the Great Escarpment of Southern Africa. J. Geophys. Res. 97, 569–585.
- Tonarini, S., Rocchi, S., Armenti, P., Innocenti, F., 1995. Constraints on timing of Ross Sea rifting inferred from Cainozoic intrusions from northern Victoria Land, Antarctica. In: Ricci, C.A. (Ed.), The Antarctic Region: Geological Evolution and Processes. Proceedings of the VII International Symposium on Antarctic Earth Sciences, Siena 1995. Terra Antarctica Publications, pp. 511–521.
- Trey, H., Makris, J., Brancolini, G., Cooper, A.K., Cochrane, G., Della Vedova, B., Acrup Working Group, 1997. The Eastern Basin Crustal model from wide-angle reflection data, Ross Sea, Antarctica. In: Ricci, C.A. (Ed.), The Antarctic Region: Geological Evolution and Processes. Proceedings of the VII International Symposium on Antarctic Earth Sciences, Siena 1995. Terra Antarctica Publications, pp. 643–648.
- Van der Beek, P., Cloetingh, S., Andriessen, P., 1994. Mechanism of extensional basin formation and vertical motions at rift flanks: constraints from tectonic modelling and fission track thermochronology. Earth Planet. Sci. Lett. 121, 417–433.
- Van der Beek, P., Andriessen, P., Cloetingh, S., 1995. Morphotectonic evolution of rifted continental margins: inferences from a coupled tectonic-surface processes model and fission track thermochronology. Tectonics 14, 406–421.
- Van der Wateren, F.M., Hindmarsh, R.C.A., 1995. East Antarctic ice sheet — stabilists strike again. Nature 376, 389–391.
- Van der Wateren, F.M., Verbers, A.L.L.M., Luyendyk, B.P., Smith, C.H., Höfle, H.C., Vermeulen, F.J.M., de Wolf, H., Herpers, U., Klas, P.W., Kubik, P.W., Suter, M., Dittrich-Hannen, B., 1996. Glaciation and deglaciation of the uplifted margins of the Cenozoic West Antarctic Rift System, Ross Sea, Antarctica. Geol. Jahrb., B 89, 123–155.
- Van der Wateren, F.M., Dunai, T.J., Klas, W., Van Balen, R.T., Verbers, A.L.L.M., Herpers, U., 1999. Contrasting Neogene denudation histories of regions in the Transantarctic Mountains, northern Victoria Land, Antarctica, constrained by cosmogenic nuclide measurements. Global Planet. Change 23, 145–172.
- Veevers, J.J., 1988. Seafloor magnetic lineation off the Otway/West Tasmania Basins: ridge jumps and subsidence history of the southeast Australian margins. Aust. J. Earth Sci. 35, 451–462.
- Watts, A.B., Karner, G.D., Steckler, M.S., 1982. Lithospheric flexure and the evolution of sedimentary basins. Philos. R. Soc. London, Ser. A, 249–281.
- Webb, P.-N., Harwood, D.M., 1991. Late Cenozoic glacial history of the Ross Embayment, Antarctica. Quat. Sci. Rev. 10, 215–223.
- Webb, P.N., Harwood, D.M., McKelvey, B.C., Scott, L.D., 1984. Cenozoic marine sedimentation and ice-volume variation on the East Antarctic craton. Geology 12, 287–291.
- Weissel, J.K., Karner, G.D., 1989. Flexural uplift of rift flanks due to mechanical unloading of the lithosphere during extension. J. Geophys. Res. 94, 13919–13950.
- White, N., 1990. Does the uniform stretching model work in the North Sea? In: Blundell, D.J., Gibbs, A.D. (Eds.), Tectonic

- Evolution of the North Sea Rifts. Clarendon Press, Oxford, pp. 217–239.
- Wilson, T.J., 1999. Cenozoic structural segmentation of the Transantarctic Mountains rift flank in southern Victoria Land. *Global Planet. Change* 23, 105–127.
- Zanolla, C., Davey, F.J., Coren, F., 1995. Seismic stratigraphic atlas of the Ross Sea, Antarctica: free air gravity anomaly map. In: Cooper, A.K., Barker, P.F., Brancolini, G. (Eds.), *Geology and Seismic Stratigraphy of the Antarctic Margin*. Antarctic Research Series 68 AGU, Washington, DC.
- Ziegler, P., 1983. Crustal thinning and subsidence in the North Sea: matters arising. *Nature* 304, 561.